2011

Comparative Study of Ethanol and Methanol Electro-oxidation on a Platinum/ceria Composite Electrode in Alkaline and Acid Solutions : Electro-catalytic Performance and Reaction Kinetics

Carlos Humberto Hidalgo Martinez
University of Central Florida

COMPARATIVE STUDY OF ETHANOL AND METHANOL ELECTRO-OXIDATION ON A PLATINUM/CERIA COMPOSITE ELECTRODE IN ALKALINE AND ACID SOLUTIONS: ELECTRO-CATALYTIC PERFORMANCE AND REACTION KINETICS

by

CARLOS HUMBERTO HIDALGO MARTINEZ
B.S. University of North Florida, 1999
M.B.A University of Phoenix, 2003

A thesis submitted in partial fulfillment of the requirements
for the degree of Master of Science
in the Department of Chemistry
in the College of Sciences
at the University of Central Florida
Orlando, Florida

Spring Term
2011

Major Professor: Diego J. Diaz

ABSTRACT

A comparative study of the electro-oxidation of ethanol and methanol was carried out on a Pt/ceria composite electrode prepared by electro-deposition. Modification of the Pt electrode was realized by co-deposition from a 1.0 mM K_2PtCl_6 solution that also contained a 20 mM suspension of ceria. The electro-catalytic activities and stabilities of the Pt/ceria catalyst towards ethanol electro-oxidation reactions (EOR) and methanol electro-oxidation reactions (MOR) were investigated by potentiodynamic and potentiostatic methods in 0.5 M sulfuric acid and 1.0 M sodium hydroxide solutions at various concentrations of ethanol and methanol. The kinetics of ethanol and methanol on a Pt/ceria composite electrode were measured in 0.5 M sulfuric acid and 1.0 M sodium hydroxide solutions using a rotating disk electrode (RDE). Cyclic voltammetry was employed in temperatures ranging from 15 to 55°C to provide quantitative and qualitative information on the kinetics of alcohol oxidation. The temperature dependence of the electro-catalytic activities afforded the determination of apparent activation energies for ethanol and methanol oxidation.

Dedicated to my wife and my parents.

Carolina, thank you for your support and motivation through these challenging years of graduate school; it would have been insurmountable without you.

To my parents, thank you for laying the foundation of success by providing exceptional secondary education and instilling perseverance, dedication, and hard work.

ACKNOWLEDGMENTS

I offer my deep and eternal gratitude to Dr. Diaz. Thank you for your guidance, knowledge, consideration and patience. Thank you for making students' learning experiences a priority. Your focus on the prime goal of graduate education instead of grants, publications, and prestige speaks volumes of your character and sets you apart from the rest.

TABLE OF CONTENTS

LIST OF FIGURES VII

LIST OF TABLES XI

1. INTRODUCTION 1

2. EXPERIMENTAL 5

2.1 REAGENTS 5
2.2 METHODS AND APPARATUS 5
2.3 PREPARATION OF MODIFIED ELECTRODES 6

3. ETHANOL ELECTRO-OXIDATION ON A PLATINUM/CERIA COMPOSITE ELECTRODE IN ACID MEDIA 7

3.1 THE BARE PLATINUM ELECTRODE AND THE TRUE SURFACE AREA OF AN ELECTRODE 7
3.2 THE PT/CERIA COMPOSITE ELECTRODE 9
3.3 EFFECT OF SCAN RATE AND ETHANOL CONCENTRATION 11
3.4 THE TEMPERATURE EFFECT 16
3.5 KINETICS 20

4. ETHANOL ELECTRO-OXIDATION ON A PLATINUM/CERIA COMPOSITE ELECTRODE IN ALKALINE MEDIA 26

4.1 THE BARE PLATINUM ELECTRODE IN 1 M SODIUM HYDROXIDE 26
4.2 THE PT/CERIA COMPOSITE ELECTRODE 27
4.3 EFFECT OF SCAN RATE AND ETHANOL CONCENTRATION 29
4.4 THE TEMPERATURE EFFECT 33
4.5 KINETICS 36

5. METHANOL ELECTRO-OXIDATION ON A PLATINUM/CERIA COMPOSITE ELECTRODE IN ACID MEDIA 40

5.1 THE PT/CERIA COMPOSITE ELECTRODE 40
5.2 EFFECT OF SCAN RATE AND METHANOL CONCENTRATION 41
5.3 THE TEMPERATURE EFFECT 44
5.4 KINETICS 46

6. METHANOL ELECTRO-OXIDATION ON A PLATINUM/CERIA COMPOSITE ELECTRODE IN ALKALINE MEDIA 50

6.1 THE PT/CERIA COMPOSITE ELECTRODE 50
6.2 EFFECT OF SCAN RATE AND METHANOL CONCENTRATION 52
6.3 THE TEMPERATURE EFFECT 55
6.4 KINETICS 58

7. CONCLUSIONS 61

8. REFERENCES 63

LIST OF FIGURES

Figure 1- Clean Pt electrode in 0.5 M H_2SO_4 Scan rate 0.1 V/s 8
Figure 2: Cyclic voltammogram for 1 M ethanol on a Pt/CeO_2 composite electrode recorded in 0.5 M H_2SO_4 electrolyte at 24 °C, scan rate 50 mV/s 10
Figure 3: Cyclic voltammograms for 1 M ethanol on Pt/CeO_2 composite electrode in 0.5 M H_2SO_4 electrolyte at 23°C. Scan rates (v) = 200, 100, 150, 50, 25 mV/sec 12
Figure 4: Peak current vs. square root of scan rate plot for 0.25M ethanol in 0.5 M H_2SO_4. Both peaks show a linear relationship with the square root of the scan rate indicating a diffusion limited reaction. 14
Figure 5: Peak current vs. square root of scan rate plot for 0.5 M ethanol in 0.5 M H_2SO_4. The peak at potential 0.7 V does not show a linear relationship linear with the square root of the scan rate indicating an adsorption process. The peak at 1.1 V has a linear relationship with the square root of the scan rate indicating a diffusion limited reaction. 14
Figure 6: Peak current vs. square root of scan rate plot for 1 M ethanol in 0.5 M H_2SO_4. The peak at potential 0.7 V is not linear with the square root of the scan rate indicating an adsorption limited reaction. The peak at 1.1 V shows a linear relationship with the square root of the scan rate indicating a diffusional process. . 15
Figure 7: Peak current vs. square root of scan rate plot for 2 M ethanol in 0.5 M H_2SO_4. The peak at potential 0.7V is not linear with the square root of the scan rate indicating an adsorption limited reaction. The peak at 1.1 V shows a linear relationship with the square root of the scan rate indicating a diffusional process. . 15
Figure 8: Cyclic voltammograms for 0.5 M ethanol on Pt/CeO_2 composite electrode in 0.5 M H_2SO_4 electrolyte at 15, 24, and 55°C. Scan rate (v) = 100 mV/sec 17
Figure 9: Arrhenius plots for 0.5 M ethanol on Pt/CeO_2 composite electrode in 0.5 M H_2SO_4 electrolyte at various potentials. Scan rate (v) = 100 mV/sec. 18
Figure 10: Activation energy vs. potential for 0.5 M ethanol in 0.5 M H_2SO_4. Scan rate 100 mV/sec. 19
Figure 11: Voltammograms of the electro-oxidation of ethanol at 0.25 M, 0.50 M, 1.0 M, and 2.0 M in 0.5 M H_2SO_4. Scan rate 100 mV/s. 20
Figure 12: Plot ln j vs. ln C for the two anodic peaks located at 0.7 V and 1.1 V in the electro-oxidation of ethanol at 0.25 M, 0.50 M, 1.0 M, and 2.0 M in 0.5 M H_2SO_4. Scan rate 100 mV/s. 22
Figure 13: Linear sweep voltammograms of 0.1 M ethanol in 0.5 M H_2SO_4 solution at the composite rotating disc electrode at sweep rate 5 mV/s with the rotation rate: 0, 300, 500, 700, 900 rpm and at 1 mV/s with the rotation rate: 250, 500, and 750 rpm. 23
Figure 14: Linear sweep voltammograms of 0.1 M ethanol in 0.5 M H_2SO_4 at a scan rate of 1 mV/s at a Pt/CeO_2 composite rotating disk electrode at 50, 250, 500, 750 rpm. 24

Figure 15: Koutecky-Levich plot of the data presented in fig. 14 for the Linear sweep voltammograms of 0.1 M ethanol in 0.5 M H_2SO_4 at a scan rate of 1 mV/s at a Pt/CeO2 composite rotating disk electrode at 50, 250, 500, 750 rpm 25
Figure 16: Clean Pt electrode in 1M NaOH Scan rate 0.1 V/s 26
Figure 17: Cyclic voltammogram for 0.5 M ethanol on a Pt/CeO_2 composite electrode recorded in 1.0 M NaOH electrolyte at 24°C, scan rate 50 mV/s..... 28
Figure 18: Cyclic voltammograms for 0.5 M ethanol on Pt/CeO_2 composite electrode in 1.0 M NaOH electrolyte at 23°C. Scan rates (v) = 200, 150, 100, 50, 25 mV/sec .. 30
Figure 19: Peak current vs. square root of scan rate plot for 0.25 M ethanol in 1 M NaOH. 31
Figure 20: Peak current vs. square root of scan rate plot for 0.5 M ethanol in 1 M NaOH. The peak at potential -0.12 V is not linear with the square root of the scan rate indicating an adsorption limited reaction..... 31
Figure 21: Peak current vs. square root of scan rate plot for 1 M ethanol in 1 M NaOH. The peak at potential -0.12 V is not linear with the square root of the scan rate indicating an adsorption limited reaction..... 32
Figure 22: Peak current vs. square root of scan rate plot for 2 M ethanol in 1 M NaOH. The peak at potential -0.12 V is not linear with the square root of the scan rate indicating an adsorption limited reaction..... 32
Figure 23: Cyclic voltammograms for 0.5 M ethanol on Pt/CeO_2 composite electrode in 1 M NaOH electrolyte at 15, 24, and 55°C. Scan rate (v) = 100 mV/sec..... 33
Figure 24: Arrhenius plots of for 0.5 M ethanol on Pt/CeO_2 composite electrode in 1 M NaOH electrolyte at various potentials. Scan rate (v) = 100 mV/sec. 34
Figure 25: Apparent activation energy vs. potential for 0.5 M ethanol in 1 M NaOH. Scan rate 100 mV/second..... 35
Figure 26: Voltammograms of the electro-oxidation of ethanol at 0.25 M, 0.50 M, 1.0 M, and 2.0 M in 1 M NaOH. Scan rate 200 mV/s..... 37
Figure 27: Plot ln j vs. ln C for the anodic peak in the electro-oxidation of ethanol at 0.25 M, 0.50 M, 1.0 M, and 2.0 M in 1 M NaOH. Scan rate 200 mV/s. 38
Figure 28: Linear sweep voltammograms of 0.1 M ethanol in 1 M NaOH solution at the composite rotating disc electrode at scan rate 5 mV/s with the rotation rate: 0, 300, 500, 700, 900, 1200, and 2000 rpm. 38
Figure 29: Cyclic voltammogram for 1 M methanol on a Pt/CeO_2 composite electrode recorded in 0.5 M H_2SO_4 electrolyte at 24 °C, scan rate 50 mV/s 40
Figure 30: Cyclic voltammograms for 0.25 M methanol on Pt/CeO_2 composite electrode in 0.5 M H_2SO_4 electrolyte at 23°C. Scan rates (v) = 200, 100, 150, 50, 25 mV/sec 41
Figure 31: Peak current vs. square root of scan rate plot for 0.25 M methanol in 0.5 M H_2SO_4..... 42
Figure 32: Peak current vs. square root of scan rate plot for 0.5 M methanol in 0.5 M H_2SO_4. The peak at potential 0.68 V is not linear with the square root of the scan rate indicating an adsorption limited reaction, which leads to poisoning of the electrode..... 43
Figure 33: Peak current vs. square root of scan rate plot for 1 M methanol in 0.5 M H_2SO_4. The peak at potential 0.68 V is not linear with the square root of the scan

rate indicating an adsorption limited reaction, which leads to poisoning of the electrode. 43
Figure 34: Cyclic voltammograms for 0.5 M methanol on Pt/CeO_2 composite electrode in 0.5 M H_2SO_4 electrolyte at 15, 24, and 55°C. Scan rate (v) = 100 mV/sec 44
Figure 35: Arrhenius plots of for 0.5 M methanol on Pt/CeO_2 composite electrode in 0.5 M H_2SO_4 electrolyte at various potentials. Scan rate (v) = 100 mV/sec. 45
Figure 36: Apparent activation energy vs. potential for 0.5 M methanol in 0.5 M H_2SO_4. Scan rate 100 mV/sec 46
Figure 37: Voltammograms of the electro-oxidation of methanol at 0.25 M, 0.50 M, 1.0 M, and 2.0 M in 0.5 M H_2SO_4. Scan rate 100 mV/s. 46
Figure 38: Plot ln j vs. ln C for the anodic peak for the electro-oxidation of methanol at 0.25 M, 0.50 M, 1.0 M, and 2.0 M in 0.5 M H_2SO_4. Scan rate 100 mV/s. 47
Figure 39: Linear sweep voltammograms of 0.1 M methanol in 0.5 M H_2SO_4 solution at the composite rotating disc electrode at sweep rate 5 mV/s with the rotation rate: 0, 200, 400, 600, 800, 1000, 1200, & 1400 rpm 48
Figure 40: Cyclic voltammogram for 1 M methanol on a Pt/CeO_2 composite electrode recorded in 1 M NaOH electrolyte at 24 °C, scan rate 50 mV/s 50
Figure 41: Cyclic voltammograms for 0.25 M methanol on Pt/CeO_2 composite electrode in 1 M NaOH electrolyte at 23°C. Scan rates (v) = 200, 100, 150, 50, 25 mV/sec. 52
Figure 42: Peak current vs. square root of scan rate plot for 0.25 M methanol in 1 M NaOH. A linear relationship with the square root of the scan rate indicates a diffusion limited reaction. 53
Figure 43: Peak current vs. square root of scan rate plot for 0.5 M methanol in 1 M NaOH. A linear relationship with the square root of the scan rate indicates a diffusion limited reaction. 53
Figure 44: Peak current vs. square root of scan rate plot for 1 M methanol in 1 M NaOH. A linear relationship with the square root of the scan rate indicates a diffusion limited reaction. 54
Figure 45: Peak current vs. square root of scan rate plot for 2 M methanol in 1 M NaOH. A linear relationship with the square root of the scan rate indicates a diffusion limited reaction. 54
Figure 46: Plot of peak current density vs. 0.25 M, 0.5 M, 1 M, and 2 M of ethanol and methanol in 0.5 M sulfuric acid and 1 M sodium hydroxide 55
Figure 47: Cyclic voltammograms for 0.5 M methanol on Pt/CeO_2 composite electrode in 1 M NaOH electrolyte at 15, 24, and 55°C. Scan rate (v) = 100 mV/sec 56
Figure 48: Arrhenius plots of for 0.5 M methanol on Pt/CeO_2 composite electrode in 1 M NaOH electrolyte at various potentials. Scan rate (v) = 100 mV/sec. 57
Figure 49: Apparent activation energy vs. potential plot for 0.5 methanol in 1 M NaOH. Scan rate 100 mV/sec 58
Figure 50: Voltammograms of the electro-oxidation of methanol at 0.25 M, 0.50 M, 1.0 M, and 2.0 M in 1 M NaOH. Scan rate 200 mV/s. 58
Figure 51: Plot ln j vs. ln C of the anodic peak for the electro-oxidation of methanol at 0.25 M, 0.50 M, 1.0 M, and 2.0 M in 1 M NaOH. Scan rate 200 mV/s. 59

Figure 52: Linear sweep voltammograms of 0.1 M methanol in 1 M NaOH solution at the composite rotating disc electrode at sweep rate 5 mV/s with the rotation rate: 0, 200, 400, 600, 800, & 1000 rpm 60

LIST OF TABLES

Table 1: Ratios of the anodic peak currents at different temperatures for the oxidation of ethanol in 0.5 M H_2SO_4 17
Table 2: Potential vs. activation energy for the electro-oxidation of ethanol in 1 M NaOH and 0.5 M H_2SO_4..... 36
Table 3: Comparison of anodic forward/reverse peak ratio of 1 M ethanol and 1 M methanol in 0.5 M H_2SO_4 and 1 M NaOH run at 50 mV/s 51

1. INTRODUCTION

A fuel cell is an electrochemical device, which transforms directly the energy of oxidation of a fuel i.e. hydrogen, natural gas, methanol, ethanol, etc, into electricity[1]. Fuel cells are similar to batteries but do not need to be recharged because instead of generating power from stored chemicals the fuel is continuously supplied[2]. The fuel is electrochemically oxidized at the anode and oxygen is electrochemically reduced at the cathode. The protons produced at the anode crossover the membrane and the electrons liberated at the anode reach the cathode through the external circuit producing an electrical energy[1]. This process does not follow the Carnot's cycle, so that higher energy efficiencies are expected: 40-50% in electrical energy, 80-85% in total energy (electricity + heat production)[1].

The concept of the fuel cell emerged in the early nineteenth century when scientists were trying to obtain a current from reverse electrolysis. The first workable fuel cell was built in 1829 by William Grove[2]. His device combined gaseous hydrogen and oxygen using platinum plates as the electrodes and sulfuric acid as the electrolyte. The fuel cell term was coined by William W. Jaques whom used phosphoric acid as an electrolyte instead of sulfuric acid[2]. Developmental research for molten carbonate and solid oxide fuel cells was conducted by Germany in the 1920's. The modern fuel cell was developed by Francis T. Bacon in 1932; he replaced the platinum electrodes with nickel and compressed the gas[2]. NASA's use of fuel cells in space to generate electrical power for spacecrafts and their groundbreaking Space Shuttle research led to the resurgence of fuel cell development[2].

Fuel cells are categorized based on the type of electrolyte it uses. These types include phosphoric acid, molten carbonate, solid oxide, alkaline, and PEM (polymer electrolyte membrane). Each fuel cell type has pros and cons in particular applications. The PEM fuel cell uses hydrogen gas as a fuel and delivers high power density and offers the advantages of low weight and volume, compared to other types[2]. However, the clean production, storage and distribution of hydrogen are still strong limitations in the use of PEMs[1]. An attractive alternative is the direct alcohol fuel cell, DAFC, because it does not require additional equipment such as a fuel reformer[3]; the relatively simple handling, storage, and transportation of the fuel because it is liquid[4]; and the high theoretical mass energy density of methanol (6.09 kWh/kg) and ethanol (8.01 kWh/kg), which is close to that of gasoline (13.3 kWh/kg)[1].

Direct methanol fuel cells, DMFC, are the most intensively investigated ones as the direct type fuel cell[3] because of its better reaction kinetics and hence better performance in a fuel cell[4]. However, DMFC are plagued with several serious problems. Methanol is toxic and highly flammable. Methanol is also easy to cross over through the Nafion membrane, causing loss of fuel and a drop in the DMFC performance. Another factor limiting the performance of a DMFC is the sluggish electro-oxidation of adsorbed carbon monoxide, an intermediate product of anodic methanol oxidation[5]. An attractive alternative is ethanol because of several advantages it holds over methanol. Ethanol has a higher energy density (8.01 kWh kg^{-1}) than methanol (6.09 kWh kg^{-1})[6]. Ethanol can be generated by fermentation of renewable raw materials containing sugar and is already widely available in its denatured form[7]. The drawback of ethanol is its poor electro-oxidation kinetics on platinum (Pt) [1], which generally is an excellent

catalyst for the oxidation of small organic molecules including ethanol[8]. In order to use the full energy density of ethanol, the fuel needs to be completely oxidized to carbon dioxide, which involves the breaking of the carbon-carbon bond[7], but due to platinum's catalytic properties, the carbon-hydrogen bond cleavage is promoted during the first adsorption steps leading to incomplete oxidation of the alcohol and intermediate products, which adsorb and thus poison the electrode. Many efforts have been made to prepare Pt catalysts in order to improve their electro-catalytic performance in ethanol oxidation[8]. These bimetallic or multi-functional electro-catalysts activate electrochemical reactions leading to an increase in the rate of fuel oxidation and oxygen reduction[1].

Examples of bimetallic and tri-metallic electro-catalysts are platinum-rhodium (PtRh), platinum-ruthenium (PtRu), platinum-tin (PtSn), and platinum-ruthenium-tin (PtRuSn). The combination of Pt with an oxophilic element is essential, since this allows for the activation of water at low potentials. This step provides oxygenated species that are necessary to oxidize some of the intermediates produced during the reaction and avoids poisoning of the catalyst surface[6]. Several metal oxides, such as RuO_2, WO_3, ZrO_2, MgO, and CeO_2, have also been used to enhance the electro-catalytical activity toward ethanol electro-oxidation through a synergistic effect. It has been suggested that the oxides are capable of adsorbing large quantities of OH species, which are involved in the oxidation/reduction mechanisms taking place between the different possible oxidation states of the metal oxides[5]. Among these, rare earth oxides exhibit a number of characteristics that make them interesting in catalytic applications, such as ceria (CeO_2)[6].

Ceria is widely regarded as a kind of oxygen tank to adjust oxygen concentration at the catalyst surface under reaction conditions[5]. Ceria has a fluorite oxide structure, where the metallic center surrounded by oxygen atoms is a cationic species capable of changing its oxidation state between +3 and +4[9]. Ceria-based catalysts have been investigated for water-gas shift reactions at low temperatures[6]. It has been reported that interaction between noble metal such as Pt with ceria enhances the catalytic activities[5]. The improved performance was attributed to the synergistic effect, and the ability of ceria to supply sufficient OH adsorbed at low potentials, which is necessary to eliminate the poisoning species especially CO adsorbed formed during the ethanol oxidation reaction[6]. Moreover, the promoting action of ceria is attributed to the higher reducibility in the presence of Pt, higher dispersion of Pt over ceria and prevention of sintering of Pt metal particles[5].

In this study, the electro-oxidation of ethanol and methanol was investigated using a Pt/ceria composite electrode prepared by electro-deposition. Modification of the Pt electrode was realized by co-deposition from a 1.0 mM K_2PtCl_6 solution that also contained a 20 mM suspension of ceria[10]. The voltammograms of the composite electrode in 0.5 M sulfuric acid and 1.0 M sodium hydroxide were first compared to the voltammograms of a bare polycrystalline platinum electrode and then its electro-catalytic activity towards the ethanol oxidation reaction (EOR) and methanol oxidation reaction (MOR) in acid and alkaline media were investigated using potentiodynamic and potentiostatic methods. Temperature effects on the EOR and MOR were also investigated.

2. EXPERIMENTAL

2.1 Reagents

Triply distilled water with 18 MΩ cm resistivity (Barnstead B-pure) was used to prepare all aqueous solutions. All chemicals were used as received. Methanol (Fisher, Anhydrous, ACS Reagent Grade) and Ethanol (Fisher, Anhydrous, ACS Reagent Grade) were used to prepare alcohol solutions of desired concentrations in 0.5 M H_2SO_4 (Fisher, ACS Reagent Grade), 0.5 M NaOH (Fisher, ACS Reagent Grade) as supporting electrolytes. High purity potassium hexachloroplatinate (Aldrich) was used for Pt electro-deposition. Ceria (cerium oxide) nanoparticles were obtained from Aldrich.

2.2 Methods and Apparatus

A three electrode apparatus was used in all electrochemistry experiments. Polycrystalline, 2 mm diameter Pt (CH Instruments, Inc.), Ag/AgCl (CH Instruments, Inc.) and Pt wire (CH Instruments, Inc.) electrodes were used as working, reference, and counter electrodes, respectively, for cyclic voltammetry and electro-deposition experiments. Cyclic Voltammetry, CV, experiments were carried out on a CH Instruments Model 760C (CH Instruments, Inc. Austin, TX) potentiostat, without regard for liquid junction. A 25 mm x 40 mm glass cell purchased from CH instruments (CHI 222) was used for the experiments. The working electrode was polished by circular rotation on a Buehler Microcloth polishing cloth, using Buehler 1 micron diamond polishing compound and Buehler Methadi fluid extender (Buehler, LTD, Lake Bluff, IL). The working electrode was then rinsed with distilled water and the cleanliness of the Pt

surface was ascertained by looking at the cyclic voltammetry of the electrode in a 0.5 M H_2SO_4 solution.

Polycrystalline, 5 mm diameter Pt rotating disk electrode (E2M Pine Research Instrumentation), Ag/AgCl (CH Instruments, Inc.) and Pt wire (CH Instruments, Inc.) electrodes were used as working, reference, and counter electrodes, respectively, for linear voltammetry. A Pine Research Instrumentation AFMSRX electrode rotator was used to perform kinetic experiments.

2.3 Preparation of Modified Electrodes

The composite electrode modified by electro-deposition was prepared by the reduction of a K_2PtCl_6 solution using a CH Instruments Model 760C potentiostat. The electro-deposition of platinum for the formation of Pt/ceria composite electrode was accomplished by holding the potential at -0.200 V vs. Ag/AgCl for 600 s while stirring the solution at rotations close to 200 rpm using a Corning PC-351 magnetic stirrer, in a slight variation of previously published results [2]. The rate of electro-deposition was kept constant by looking at the current while depositing and adjusting the potential accordingly in order to keep the current constant.

The cleanliness and suitability of the electrode prior to any electrochemical oxidation of the alcohols was ascertained by looking at the cyclic voltammetry of a 0.5 M H_2SO_4 solution using the desired electrode. All cyclic voltammetry experiments were carried at a scan rate of 100 mV/s unless specified. Moreover, the currents observed for the hydrogen adsorption regions of the voltammogram were used for normalization of the electro-active surface area of the electrodes after modification.

3. ETHANOL ELECTRO-OXIDATION ON A PLATINUM/CERIA COMPOSITE ELECTRODE IN ACID MEDIA

3.1 The Bare Platinum Electrode and the True Surface Area of an Electrode

Figure 1 show the cyclic voltammogram (CV) of a bare, clean Pt electrode recorded in a 0.5 M solution of H_2SO_4. The CV curve presents three separate regions of a Pt electrode in sulfuric acid. The first region is known as the oxygen region found at positive potentials between 0.3 V and 1.25 V where platinum oxides are formed. The next region is known as the double layer region, which encompasses the full potential range for the electrode. The double layer region present lower currents that are found to be mostly due to capacitive processes that take place at the electrode/solution interface. The double layer is prominently observed between 0.15 V and 0.25 V because of the absence of other redox processes such as the platinum oxidation and hydrogen reduction in this range. Finally, the third region is known as the chemisorbed hydrogen region found at negative potentials between -0.1 V to 0.1 V. One would expect three peaks in this area because the Anderson criterion proposes that in a polycrystalline surface the lower Miller index planes (100), (110), and (111) predominate in a proportion of 33% for each one[11]. However, the poorly defined or missing peak is probably due to the competitive adsorption of bisulfate anions from the sulfuric acid solvent [11].

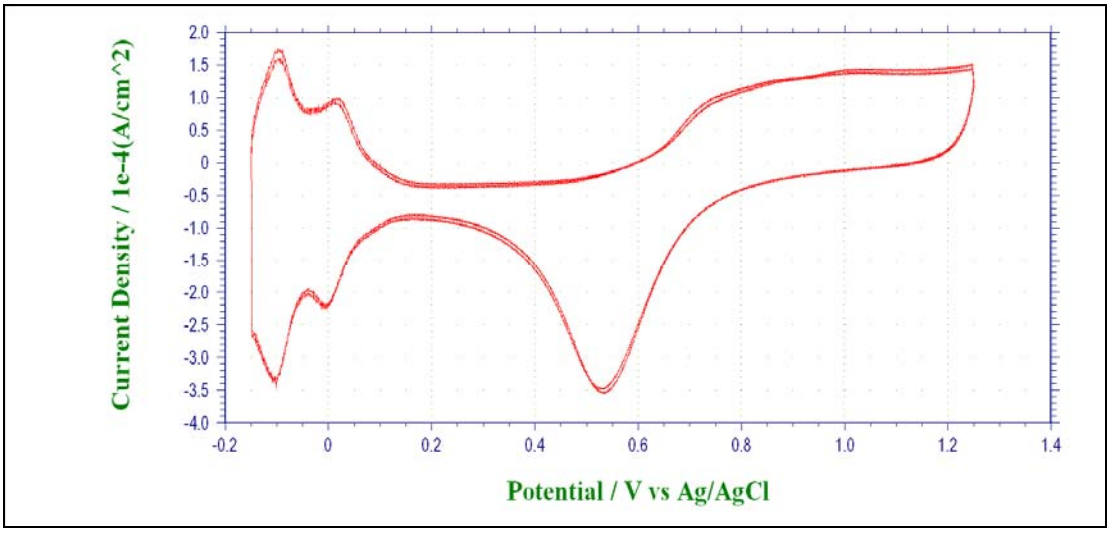

Figure 1- Clean Pt electrode in 0.5 M H_2SO_4 Scan rate 0.1 V/s

The chemisorbed hydrogen region can be used to determine the true surface area of a platinum electrode. It is important to know the true surface area of an electrode because the total amount of current observed at an electrode surface will be proportional to not only the concentration of electro-active species, but also to the number of surface sites available for charge transfer to occur. Thus, the observed reaction rate, and consequently the total amount of electric current, is proportional to the electrode's real surface area [11]. The surface of an electrode might appear flat and smooth on the macroscopic scale, but the cleaning and polishing of the surface makes the electrode rough and uneven in the microscopic scale, leading to a larger surface area compared to what would be predicted from the geometric surface area. It is thus necessary to use the hydrogen chemisorbtion region in order to determine the true surface area of the electrode.

When a hydrogen atom is adsorbed on a platinum surface, a charge-transfer process occurs which involve one electron per hydrogen atom, such that for one mole (n_a) of hydrogen atoms:

$$n_a = Q_m/F \quad (1)$$

where F is Faraday's constant and Q_m is the charge associated with the formation of a monolayer. Real surface area can be calculated using the equation:

$$S_r = (n_a N_A)/d_m \quad (2)$$

where N_A is Avogadro's number and d_m is the surface atom density of the theoretically smooth metal from crystallographic data, and has a value of 1.3×10^{15} cm^{-2}. Substituting equation 1 into equation 2 gives:

$$S_r = Q_m/e\ d_m \quad (3)$$

Where e is the electron charge (1.602×10^{-19} C) giving the denominator a constant value of 208 μC/ cm^2. Q_m is evaluated by integrating the area under the curve of the chemisorbtion region using the potentiostat's software tools. The value obtained by the software is divided by 208 μC/ cm^2 to obtain the real surface area of the electrode, which should always be equal to or greater than the geometric surface area of the electrode. The geometric surface area of the electrode is 0.0314 cm^2.

As the total amount of current observed at the electrode surface is proportional to the electrode's true surface area, this area of the electrode is also used to normalize the current. Current density is current divided by the true surface area of the electrode. This allows the comparison of current produced per unit area, and the area is in centimeters square.

3.2 The Pt/ceria Composite Electrode

The cyclic voltammogram of the electro-oxidation of a 1 M solution of ethanol at a Pt/CeO_2 composite electrode in 0.5 M H_2SO_4 electrolyte is shown in Figure 2 and was

in good agreement with those obtained for the electro-oxidation of ethanol at a polycrystalline Pt electrode [12] with regards to the shape of the curve demonstrating two peaks in the forward anodic scan and one peak in the reverse cathodic scan. The oxidation of ethanol in acid solution proceeds in two parallel reaction mechanisms. The first anodic peak represents the complete oxidation of the fuel to carbon dioxide (CO_2) and the second anodic peak represents the partial oxidation of the alcohol to acetic acid. The formation of CO_2 goes through two types of adsorbed intermediates, which are fragments with one and two carbon atoms. There is no agreement regarding the nature of the adsorbed species [13]. According to some researchers, the carbon-carbon bond is preserved, but others claim that the main intermediates contain only one carbon atom. Controversy also exists on whether acetic acid is formed in one step or through the acetaldehyde [13].

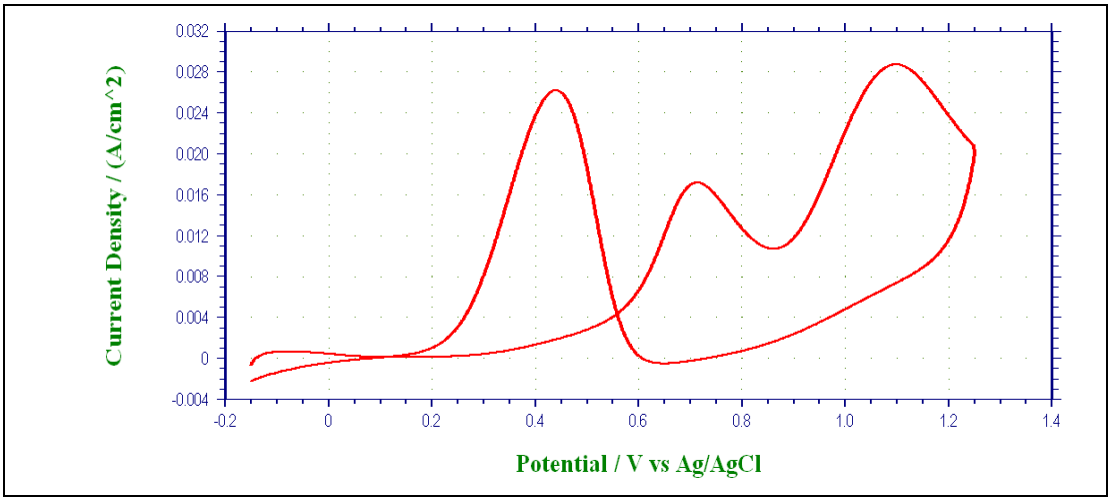

Figure 2: Cyclic voltammogram for 1 M ethanol on a Pt/CeO_2 composite electrode recorded in 0.5 M H_2SO_4 electrolyte at 24 °C, scan rate 50 mV/s

At the Pt/CeO_2 composite electrode, the onset potential or the voltage at which oxidation begins, was approximately 0.35 V vs Ag/AgCl. During the positive sweep, two oxidation peaks appear approximately at 0.7 and 1.1 V vs. Ag/AgCl. The appearance of

two peaks on the anodic sweep can be ascribed to the oxidation of the fuel by two kinds of chemisorbed oxygen species. A surface layer of Pt-OH is first formed on Pt at around 0.4 V vs. Ag/AgCl and this is subsequently transformed into a Pt-O layer in the region of 1.0 V vs. Ag/AgCl[14]. During the negative sweep, ethanol oxidation currents set in with the reduction of the platinum oxide negative of circa 0.6 V vs. Ag/AgCl and decreases again at more negative potentials due to re-poisoning of the catalyst. The overall current of the modified (Pt/ceria) electrode was higher compared to the bare polycrystalline Pt electrode. The current densities obtained with the composite electrode were 0.024 A/cm^2 for the peak at potential 0.7 V vs. Ag/AgCl and 0.030 A/cm^2 for the peak at potential 1.1 V vs. Ag/AgCl. The current density of the forward scan peaks obtained with a bare Pt electrode were 0.002 A/ cm^2 for the first peak in the forward scan and 0.0025 A/ cm^2 for the second peak. Diaz et. al. proposed two mechanisms for the higher current density obtained with the composite electrodes. The cerium oxide may be inhibiting CO adsorption or the ceria's oxygen storage capacity is facilitating the oxidation of adsorbed carbon monoxide [10].

3.3 Effect of Scan Rate and Ethanol Concentration

Figure 3 shows the electro-oxidation of ethanol in 0.5 M sulfuric acid at five different scan rates: 25, 50, 100, 150, 200 mV/s. The electrochemical oxidation of ethanol at different scan rates was studied in order to qualitatively observe possible adsorption of redox species on the electrode surface and their kinetics effects on the rate-determining step. By solving the Fick's laws of diffusion for mass transport into a planar electrode it has been demonstrated that the total current on a electrode will be

proportional to the scan rate if the redox species are adsorbed on the electrode surface, whereas it will be proportional to the square root of the scan rate for a fully diffusional process [15].

The cyclic voltammetry studies were also carried at different concentrations of ethanol. The CVs obtained at different concentration and scan rate can provide information on the time dependence and rates of the different processes contributing to the total reaction rate [16].

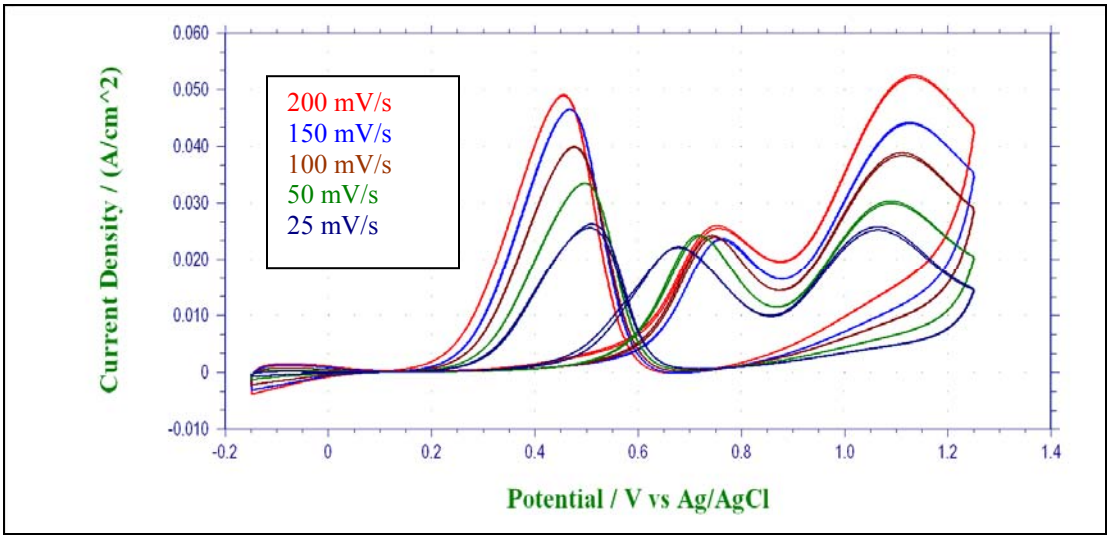

Figure 3: Cyclic voltammograms for 1 M ethanol on Pt/CeO_2 composite electrode in 0.5 M H_2SO_4 electrolyte at 23°C. Scan rates (v) = 200, 100, 150, 50, 25 mV/sec

For the oxidation of a 1 M ethanol solution it was observed that with increasing scan rate, the peak at potential 0.7 V shifted to a more positive potential except for the 200 mV/s scan rate, which remains at the same potential as the 100 mV/s scan rate. The peak currents for this first peak in the forward scan do not increase linearly with the square root of the scan rate indicating an adsorptive process[17]. The second peak in the forward scan located at potential 1.1 V did not shift in any direction with increasing scan rate and the peak currents increased linearly with the square root of the scan rate as would

be expected for a diffusion limited reaction. This same pattern was observed when the ethanol concentration was changed to 0.5 and 2 M. When the ethanol concentration was reduced to 0.25 M, the current of the two anodic peaks increased linearly with the square root of the scan rate. Current vs. square root of the scan rate plots for the different concentrations are shown in figures 4, 5, 6, and 7.

The main adsorbed intermediates for the total oxidation of ethanol contain only one carbon atom namely carbon monoxide (CO). The adsorption of CO, and poisoning of the electrode, was seen in the deviation from linearity between the current and the square root of the scan rate for the first peak (0.7 V) at every concentration. At high concentrations, there is more CO thus more adsorption and slower desorption. At low concentrations, there is sufficient time for the CO to desorb, thus the linear relationship observed in the first peak at 0.25 M may initially lead to the incorrect assumption that the process is diffusional when in fact it is adsorptive. The second peak, (1.1 V), which represents the formation of acetic acid, is a diffusional process thus the electrode was not being poisoned. However, the partial oxidation of the alcohol lowers the fuel's capacity to generate electricity because ethanol oxidation to acetic acid is a 4 electron process as opposed to 12 electrons per ethanol molecule obtained when ethanol is completely oxidized to carbon dioxide.

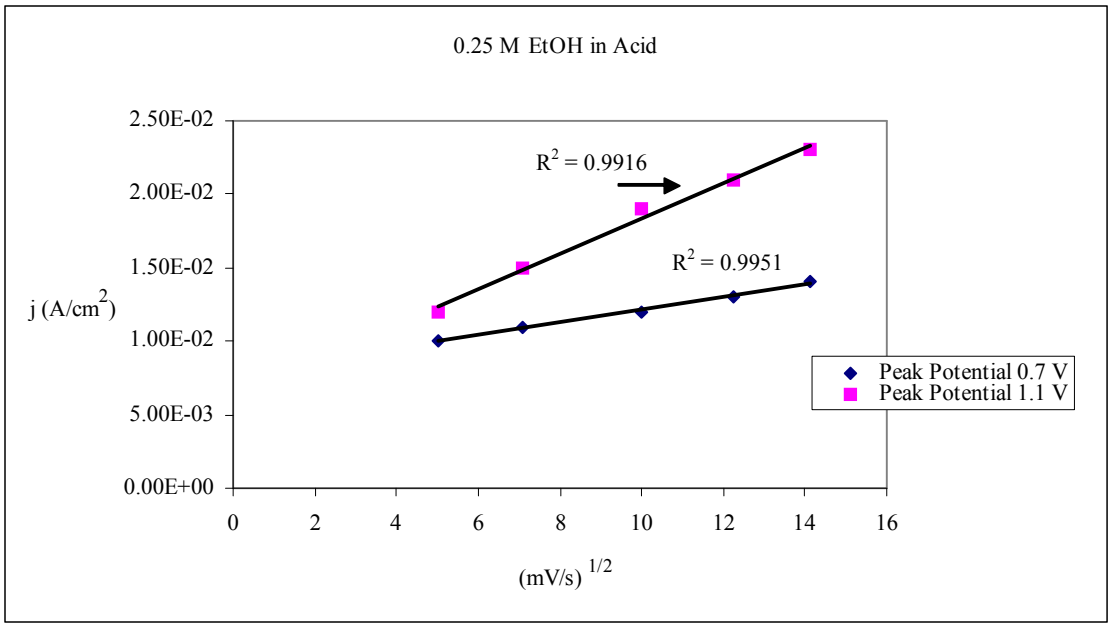

Figure 4: Peak current vs. square root of scan rate plot for 0.25 M ethanol in 0.5 M H_2SO_4. Both peaks show a linear relationship with the square root of the scan rate indicating a diffusion limited reaction.

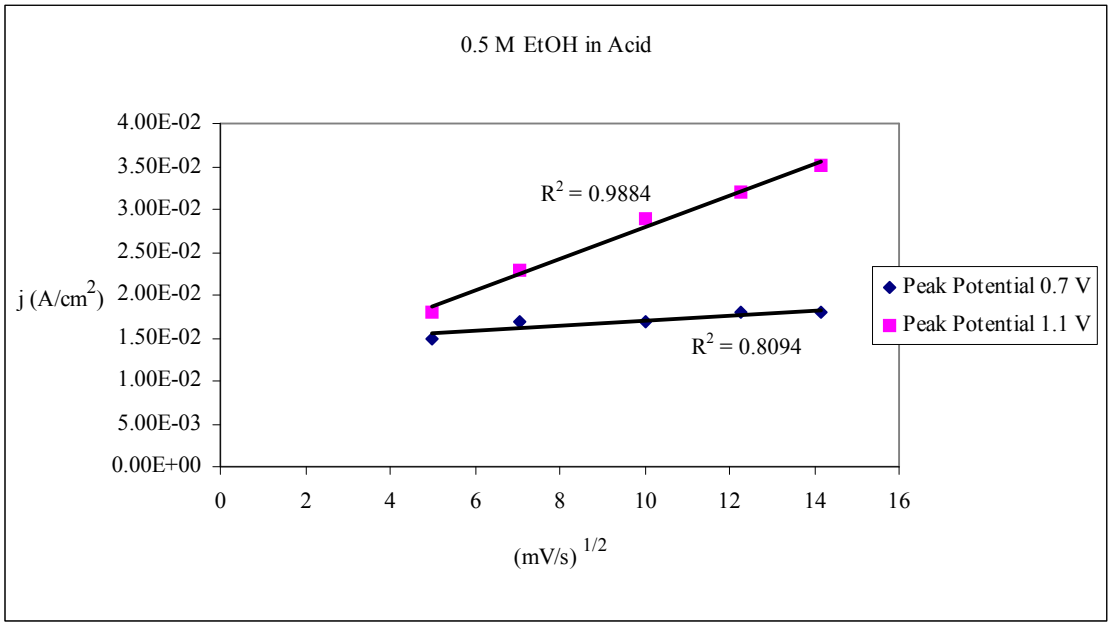

Figure 5: Peak current vs. square root of scan rate plot for 0.5 M ethanol in 0.5 M H_2SO_4. The peak at potential 0.7 V does not show a linear relationship linear with the square root of the scan rate indicating an adsorption process. The peak at 1.1 V has a linear relationship with the square root of the scan rate indicating a diffusion limited reaction.

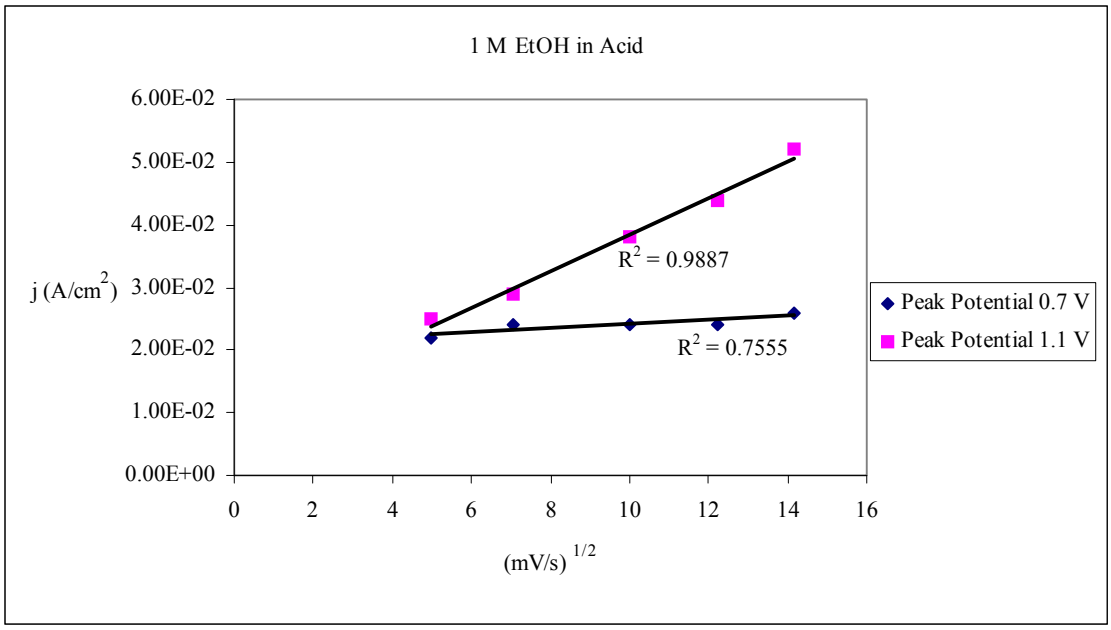

Figure 6: Peak current vs. square root of scan rate plot for 1 M ethanol in 0.5 M H_2SO_4. The peak at potential 0.7 V is not linear with the square root of the scan rate indicating an adsorption limited reaction. The peak at 1.1 V shows a linear relationship with the square root of the scan rate indicating a diffusional process.

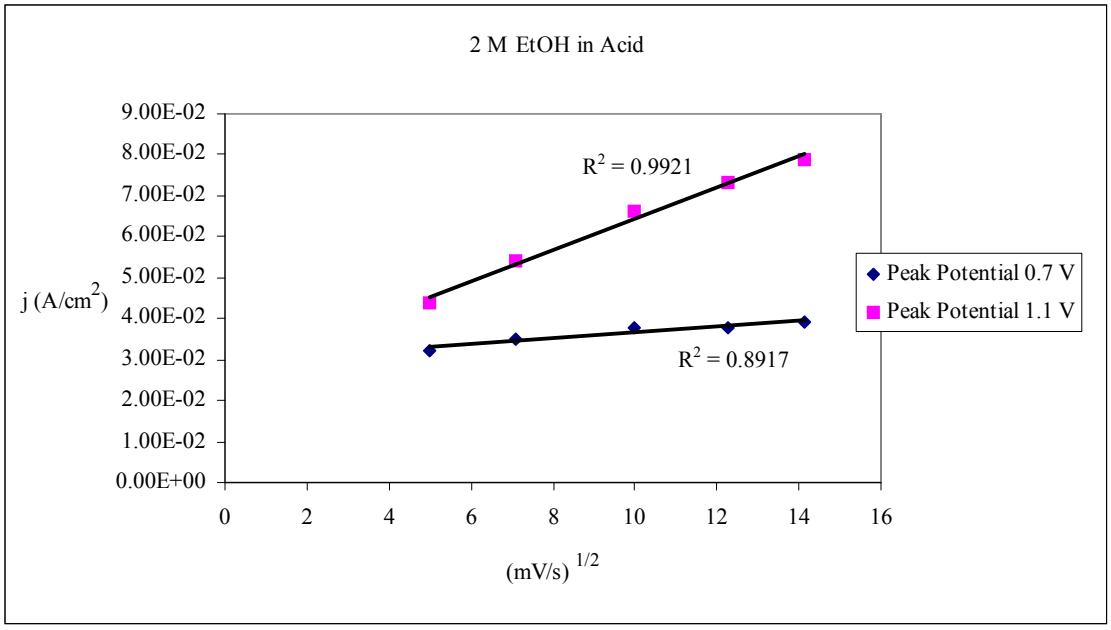

Figure 7: Peak current vs. square root of scan rate plot for 2 M ethanol in 0.5 M H_2SO_4. The peak at potential 0.7V is not linear with the square root of the scan rate indicating an adsorption limited reaction. The peak at 1.1 V shows a linear relationship with the square root of the scan rate indicating a diffusional process.

The dependence of the peak potential on the scan rate also provides kinetic information [18]. A peak potential that is independent of the scan rate indicates a reversible charge transport process, whereas an irreversible charge transfer process causes the peak potential to vary with scan rate [17]. The peak at potential 0.7 V shows a dependence on the scan rate indicating irreversibility in the charge transfer process. The peak at potential 1.1 V was independent of the scan rate indicating a reversible charge transport process. It should be noted that the reversibility aforementioned refers to electrochemical reversibility and should be distinguished from thermodynamic reversibility. The latter occurs when an infinitesimal reversal in a driving force causes a change in direction and a continuous state of equilibrium exists. When a state of equilibrium exists between the reductant and oxidant at the surface of an electrode and the Nernst equation can be applied then the reaction is considered to be electrochemically reversible because it obeys the conditions of thermodynamic reversibility. In an electrochemical irreversible process, the reaction at the electrode can not be reversed because of a high kinetic barrier; however, this does not mean that a state of equilibrium exists at the electrode surface so while the process is electrochemically irreversible it may be thermodynamically reversible.

3.4 The Temperature Effect

Figure 8 is the I-V curves for the electro-oxidation reaction on Pt/CeO_2 composite electrode in 0.5 M sulfuric acid containing 0.5 M ethanol at temperatures 15, 24, and 55°C.

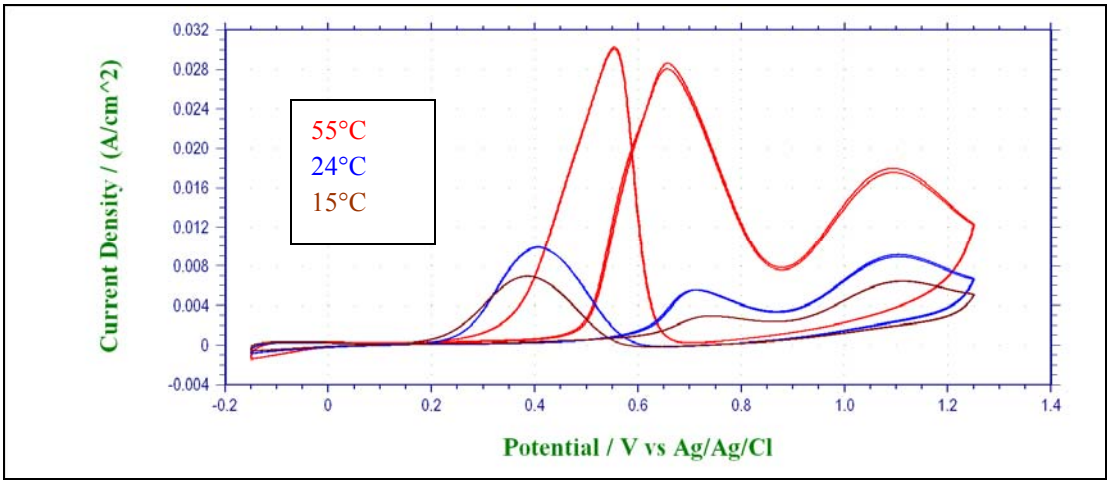

Figure 8: Cyclic voltammograms for 0.5 M ethanol on Pt/CeO_2 composite electrode in 0.5 M H_2SO_4 electrolyte at 15, 24, and 55°C. Scan rate (v) = 100 mV/sec

The electro-catalytic activity of the composite electrode was enhanced as evidenced by the negative shift of the onset potential and increase in oxidation current with increasing temperature. The first peak in the forward scan located at 0.7 V vs. Ag/AgCl became sharper indicating improved reaction kinetics at the higher temperature. The second peak at 1.1 V vs. Ag/AgCl was larger than the first peak at low and ambient temperatures but at 55°C an inversion occurred and the second peak became approximately half of the first peak demonstrating a preference toward that mechanism. The ratio of the peak currents for peak 1 to peak 2 at each temperature were calculated and are shown in table 1.

Table 1: Ratios of the anodic peak currents at different temperatures for the oxidation of ethanol in 0.5 M H_2SO_4

Peak Current Ratios at Different Temperatures			
T	i_p at 0.7 V	i_p at 1.1 V	Peak ratio
°C	A	A	
15	0.00296	0.00649	0.46
24	0.00549	0.00903	0.61
55	0.02830	0.01770	1.60

Figure 9 shows Arrhenius plots for the current densities obtained from the oxidation of ethanol in 0.5 M sulfuric acid on a Pt/CeO_2 composite electrode at different temperatures and various potentials.

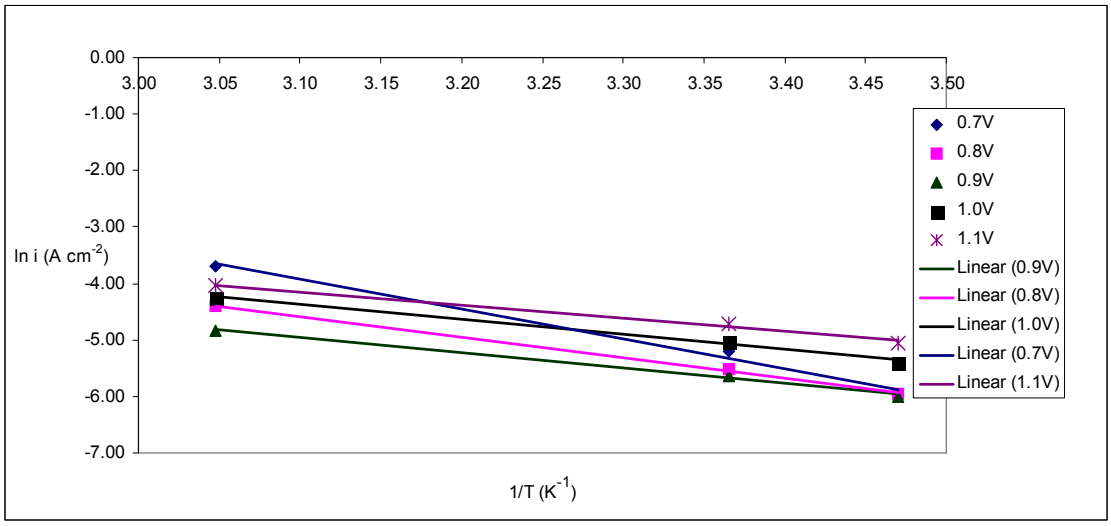

Figure 9: Arrhenius plots for 0.5 M ethanol on Pt/CeO_2 composite electrode in 0.5 M H_2SO_4 electrolyte at various potentials. Scan rate (v) = 100 mV/sec.

Linear relationships were obtained at the various potentials when ln i vs. the reciprocal of the temperature was plotted. This is evidence that the mechanism at each potential is not changing with temperature. The slope (m) of the linear curves obtained in figure 9 is equal to

$$m = - E_{app} / R \quad (4)$$

where E_{app} is the apparent activation energy and R is the universal gas constant (8.314 J K^{-1} mol^{-1}). The apparent activation energy can be calculated by rearranging the slope equation

$$E_{app} = mR \quad (5)$$

The activation energy of ethanol is referred to as apparent because the value includes reaction intermediates such as the formation of acetic acid and acetaldehyde.

The apparent activation energies at 0.7 V, 0.8 V, 0.9 V, 1.0 V, and 1.1 V were 43.6, 30.3, 22.5, 21.9, and 19.3 kJ/mol, respectively. Hariyanto et. al. reported the average activation energies for the overall electro-oxidation reaction at a $PtCeO_2/C$ and Pt/C catalyst in 0.5 M sulfuric acid at about 29 and 30.5 kJ/mol, respectively [19]. The apparent activation energies were plotted against potential in figure 10.

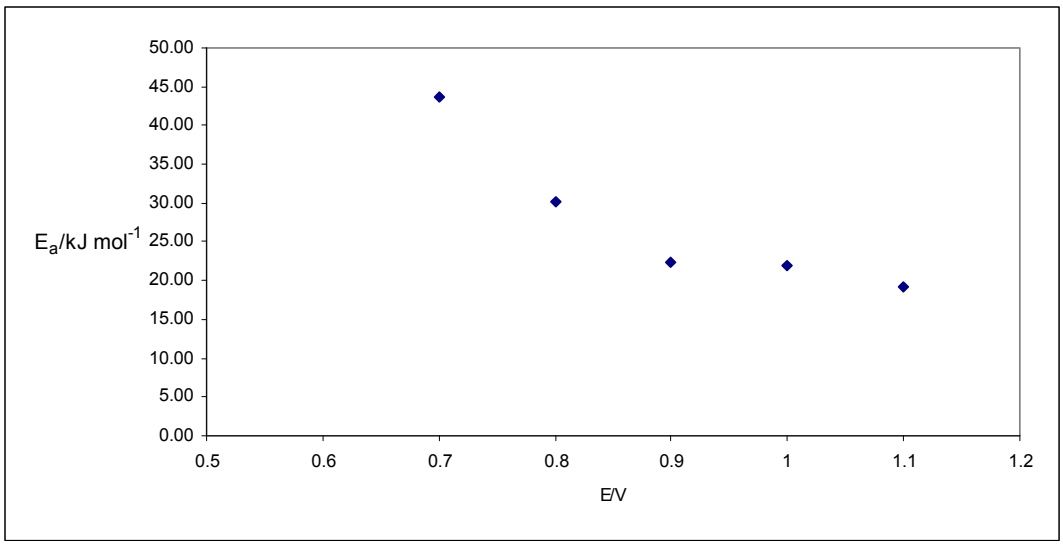

Figure 10: Activation energy vs. potential for 0.5 M ethanol in 0.5 M H_2SO_4. Scan rate 100 mV/sec.

The plot shows a strong dependence of the activation energy on the electrode potential, which was not surprising since the total oxidation of the alcohol, the transfer of 12 electrons, occurs at approximately 0.7 V. Oxidation of ethanol to the acetaldehyde and acetic acid intermediates occurs at approximately 1.1 V and since this process only involves the transfer of 2 and 4 electrons, respectively, the activation energy required was much smaller and thus preferred. An exception was seen at 55°C where more of the alcohol was being completely oxidized. The higher temperature provides the additional energy needed for the complete oxidation of ethanol.

3.5 Kinetics

The electro-oxidation of various ethanol concentrations in 0.5 M sulfuric acid is shown in figure 11.

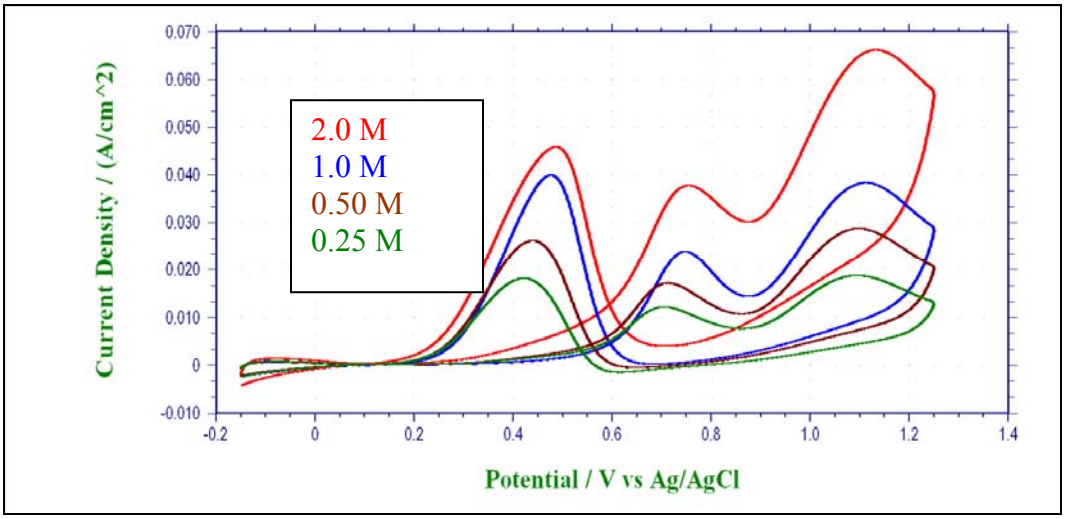

Figure 11: Voltammograms of the electro-oxidation of ethanol at 0.25 M, 0.50 M, 1.0 M, and 2.0 M in 0.5 M H_2SO_4. Scan rate 100 mV/s.

As the ethanol concentration increases, the peak current densities of all peaks increase. The peaks also shift slightly positive as the concentration increases. In comparing the peak current densities of the 2 M ethanol solution (0.0377 A/cm^2 first anodic peak and 0.0664 A/cm^2 second anodic peak) to the current densities of the 0.25 M ethanol solution (0.0124 A/cm^2 first anodic peak and 0.0189 A/cm^2 second anodic peak), a decrease of almost 1 order of magnitude, there was an approximate 3 fold decrease in oxidation current, which may indicate that the overall electro-oxidation rate is controlled by surface processes rather than by pure mass transport. The anodic current can be expressed as

$$I = nF\upsilon \quad (6)$$

Where n is the number of electrons, F the Faraday constant and υ the reaction rate, with:

$$\upsilon = kCm \quad (7)$$

where k is the rate constant, C the bulk concentration of the reactant and m the overall reaction order. Substituting the reaction rate into the anodic current formula and normalizing by dividing by the true surface area (A) of the electrode gives:

$$j = (nFk/A)\, Cm \quad (8)$$

Taking the natural log of both sides gives:

$$\ln j = \ln(nFK/S) + m \ln C \quad (9)$$

The slope of a linear relationship between ln j and ln C represents the overall reaction order, m [20].

The plot of the natural logarithm of the current densities vs. the natural logarithm of the concentration of the two anodic peaks is shown in figure 12. Thus, at 0.7 V, m = 0.5 and at 1.1 V, m = 0.6. The reaction seems to be controlled by a half order process for the two anodic peaks. Hitmi et al. [20] reported an overall reaction order of 0.7 at 0.6 V Ag/AgCl on a polycrystalline Pt electrode and Wang et al. [4] reported an overall order of 0.6 at the same potential on a polycrystalline Pt electrode.

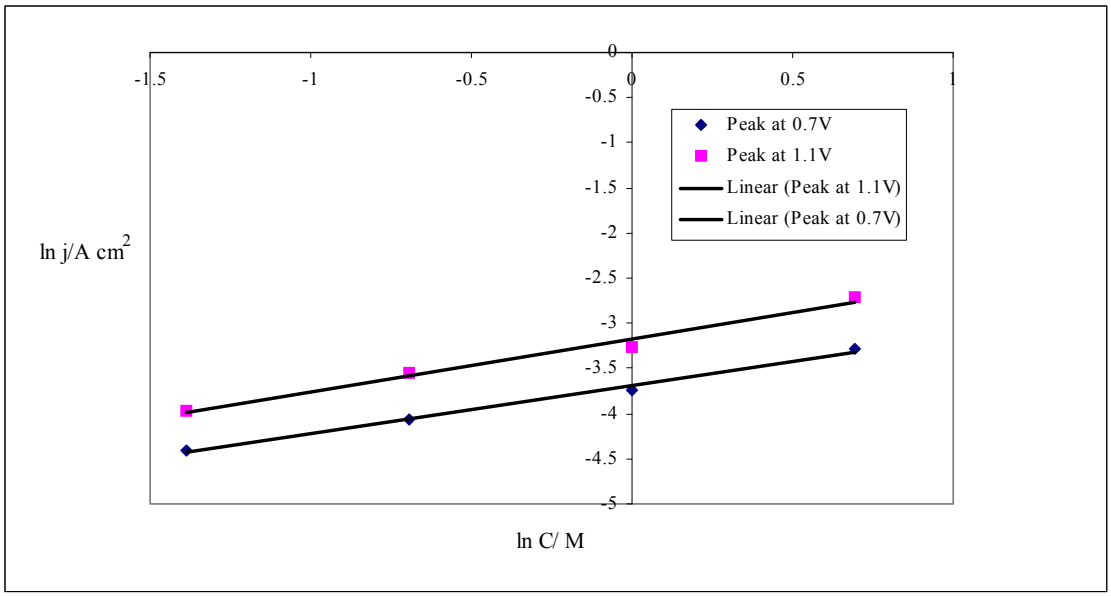

Figure 12: Plot ln j vs. ln C for the two anodic peaks located at 0.7 V and 1.1 V in the electro-oxidation of ethanol at 0.25 M, 0.50 M, 1.0 M, and 2.0 M in 0.5 M H_2SO_4. Scan rate 100 mV/s.

Figure 13 shows the linear sweeping voltammograms of 0.1 M ethanol in 0.5 M H_2SO_4 solution on the composite rotating disk electrode (RDE) at 1 and 5 mV/s scan rates and different rotation rates. The RDE is vertically mounted in the shaft of a synchronous controllable-speed motor and rotated with constant angular velocity (ω) about an axis perpendicular to the plain disk surface ($\omega = 2\pi f$, where f is the rotation speed in revolutions per second, rps). As a result of this motion, the solution in an adjacent layer develops a radial velocity that moves it away from the disk center. This solution is replenished by a flow normal to the surface. Hence, the RDE can be viewed as a pump that draws a fresh solution up from the bulk solution at a controlled flow rate [21]. The peak current density increased when the rotation rate was increased from 0 to 300 rpm indicating a mass transport limited process. When the rotation rate was further increased to 500 rpm, the peak current density decreased indicating a kinetically limited process. Further increases in the rotation rate did not cause the current density to

decrease, but rather remained constant. However, when the scan rate was lowered from 5 mV/s to 1 mV/s, the peak current density decreased further confirming the kinetically limited process.

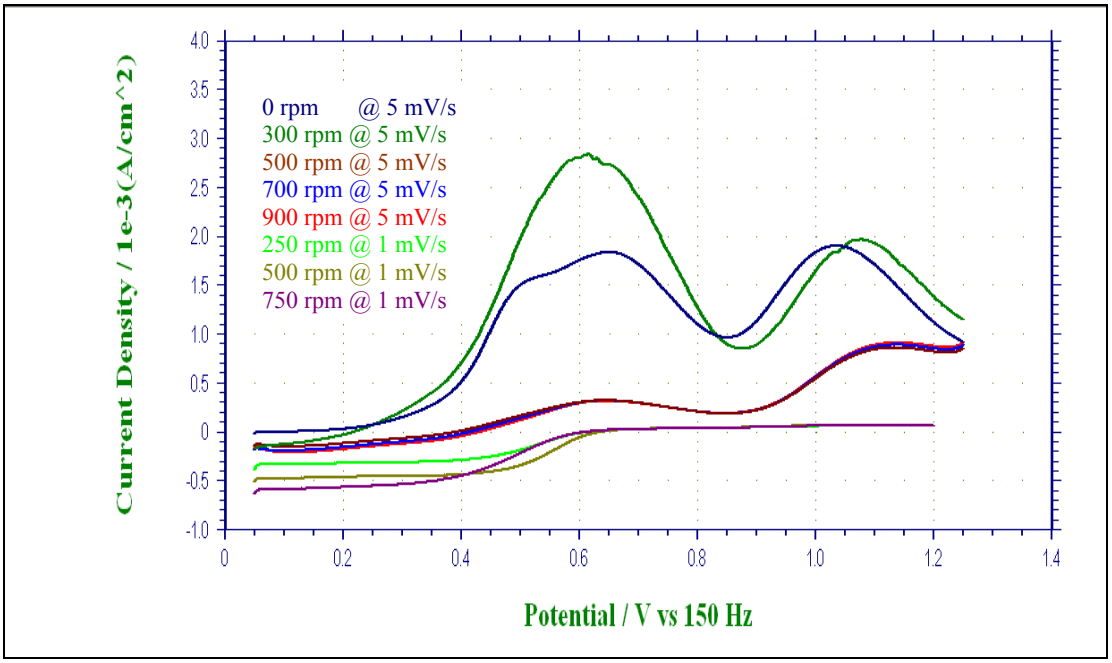

Figure 13: Linear sweep voltammograms of 0.1 M ethanol in 0.5 M H_2SO_4 solution at the composite rotating disc electrode at sweep rate 5 mV/s with the rotation rate: 0, 300, 500, 700, 900 rpm and at 1 mV/s with the rotation rate: 250, 500, and 750 rpm.

Since both mass transfer and kinetic components are involved in the oxidation of ethanol, a Koutechy-Levich plot was used to further study the irreversible electrode reaction. The total current (i) can be mathematically stated as

$$1/i = 1/i_k + 1/i_d \quad (10)$$

where i_k is the kinetic current and is defined as

$$i_k = nFk_f[C_2H_6O] \quad (11)$$

where $[C_2H_6O]$ is the bulk concentration of ethanol, n is the number of electrons transferred, F is Faraday's constant and k_f is the heterogeneous electron transfer rate. The kinetic current represents the current in the absence of any mass transfer effects, that is,

the current that would flow under the kinetic limitation if the mass transfer were efficient enough to keep the concentration at the electrode surface equal to the bulk value [17]. The diffusion current, i_d, is given by

$$i_d = 0.62nF[C_2H_6O]\omega^{1/2}\upsilon^{-1/6}D^{2/3} \quad (12)$$

where $D^{2/3}$ is the diffusion coefficient, υ is the kinematic viscosity, which for a dilute solution is 0.01 cm^2/s, and ω in rad/s. The diffusional current which is proportional to the limiting current applies to the totally mass-transfer limited condition at the RDE [17]. Thus, for kinetic and mass transfer controlled reactions a Koutechy-Levich plot of 1/i vs. $1/\omega^{1/2}$ should result in a linear relationship from which the kinetic current and diffusion coefficient may be evaluated [22]. Figure 14 is the linear sweep voltammograms of 0.1 M ethanol in 0.5 M H_2SO_4 at a scan rate of 1 mV/s. Figure 15 displays the Koutecky-Levich plot for the experimental data shown in figure 14.

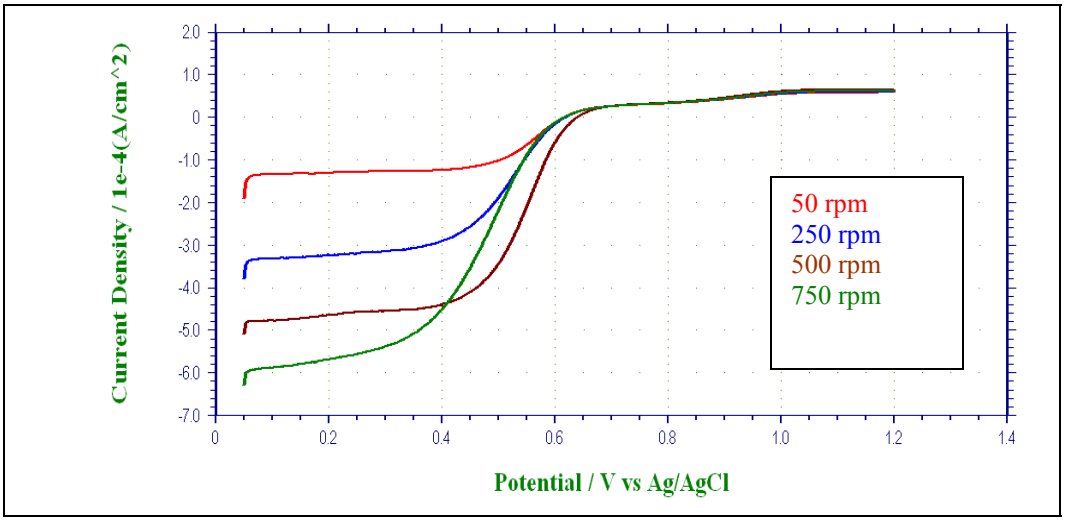

Figure 14: Linear sweep voltammograms of 0.1 M ethanol in 0.5 M H_2SO_4 at a scan rate of 1 mV/s at a Pt/CeO_2 composite rotating disk electrode at 50, 250, 500, 750 rpm.

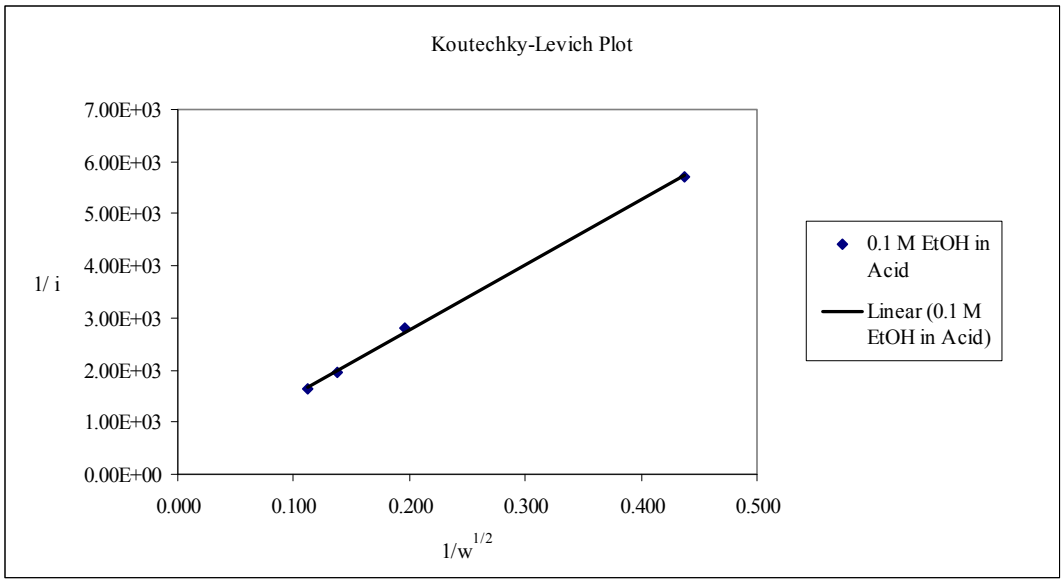

Figure 15: Koutecky-Levich plot of the data presented in fig. 14 for the Linear sweep voltammograms of 0.1 M ethanol in 0.5 M H_2SO_4 at a scan rate of 1 mV/s at a Pt/CeO2 composite rotating disk electrode at 50, 250, 500, 750 rpm

A linear relationship was observed with current increasing with increasing rotation rate. Extrapolating $\omega^{-½}$ to zero gives $1/i_k$ and its reciprocal is the kinetic current, which was 3.92 mA/cm^2. The diffusional current, which is equal to the reciprocal of the slope, was 0.08 mA/cm^2 and the diffusional coefficient was 5.56 x 10^{-12} cm^2/s. The kinetic process was contributing more to the overall current than the diffusional process. The standard rate constant for a 1 electron transfer was 4.06 x 10^{-4} cm/s. This value, neither large nor small, indicates more of a quasi-reversible reaction than an irreversible reaction at the Pt/CeO_2 composite electrode, which supports the results obtained from the data presented in this chapter.

4. ETHANOL ELECTRO-OXIDATION ON A PLATINUM/CERIA COMPOSITE ELECTRODE IN ALKALINE MEDIA

4.1 The Bare Platinum Electrode in 1 M Sodium Hydroxide

Figure 16 is the base cyclic voltammogram (CV) of a Pt electrode recorded in a 1 M solution of sodium hydroxide (NaOH).

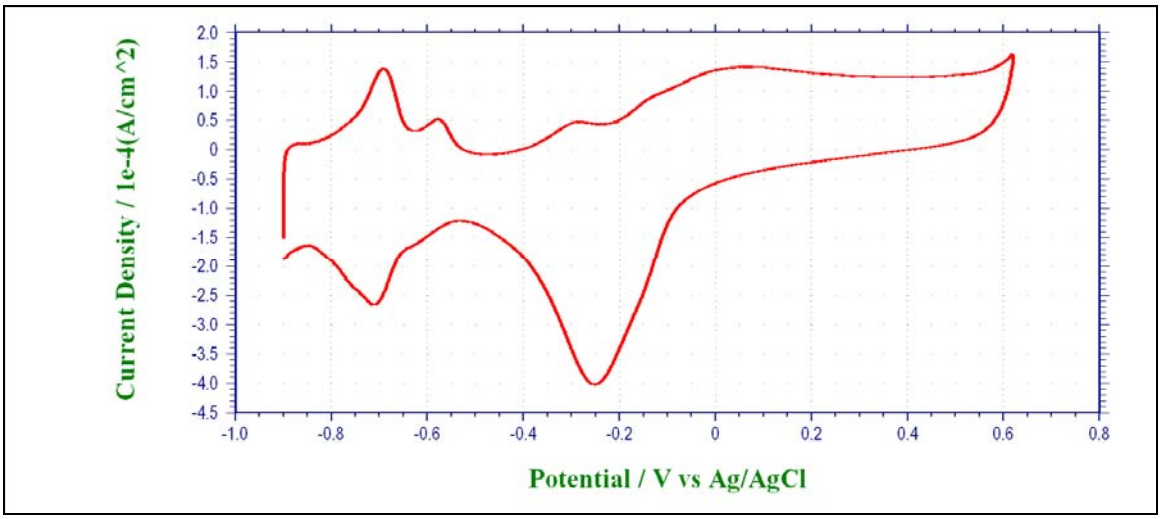

Figure 16: Clean Pt electrode in 1 M NaOH Scan rate 0.1 V/s

The cyclic voltammogram was similar in shape to that of the CV of a platinum electrode in 0.5 M sulfuric acid. A notable difference between the CV of the platinum electrode in alkaline media and the CV of the platinum electrode in acid media was that in the alkaline media the CV shifts to a negative potential of approximately 0.6 V. This is explained by using a special form of the Nernst equation

$$E = E° - (59.2\ mV/n) \log Q \quad (13)$$

where Q is the reaction concentration quotient and n is the number of electrons transferred. The standard oxidation potential of hydrogen is

$$\tfrac{1}{2}H_2(g) \Rightarrow H^+(aq) + e^- \qquad E° = 0 \quad (14)$$

substituting the hydrogen standard potential in the Nernst equation gives

$$E = -(59.2\ mV) \log [H^+]/P_{H_2}^{½} \quad (15)$$

at 1 atm of pressure, the equation is

$$E = -(59.2\ mV) \log [H^+] \quad (16)$$

since the pH of a solution is given by

$$pH = - \log [H^+] \quad (17)$$

therefore

$$E = (59.2\ mV)\ pH \quad (18)$$

This equation shows that potential is directly proportional to pH. If pH increases by 1 unit then the potential will increase by 59.2 mV or in other words as the hydrogen concentration decreases the potential will shift in a negative direction.

A second difference between the CV of a platinum electrode in acid and base are the well defined hydrogen peaks in the basic media, which can be attributed to the fact that there are no other ions competing for adsorption sites on the platinum electrode surface. A final difference between the two cyclic voltammograms was a less prominent double layer, which is due to less adsorption as less capacitance is due to adsorbed anions. The hydrogen desorption region is immediately followed by the hydroxide adsorption region.

4.2 The Pt/ceria Composite Electrode

The cyclic voltammogram of the electro-oxidation of a 0.5 M solution of ethanol at a Pt/CeO_2 composite electrode in 1.0 M NaOH electrolyte is shown in Figure 17 and was in good agreement with those obtained for the electro-oxidation of ethanol at a

polycrystalline Pt electrode [23] with one peak in the forward anodic scan and one peak in the reverse cathodic scan.

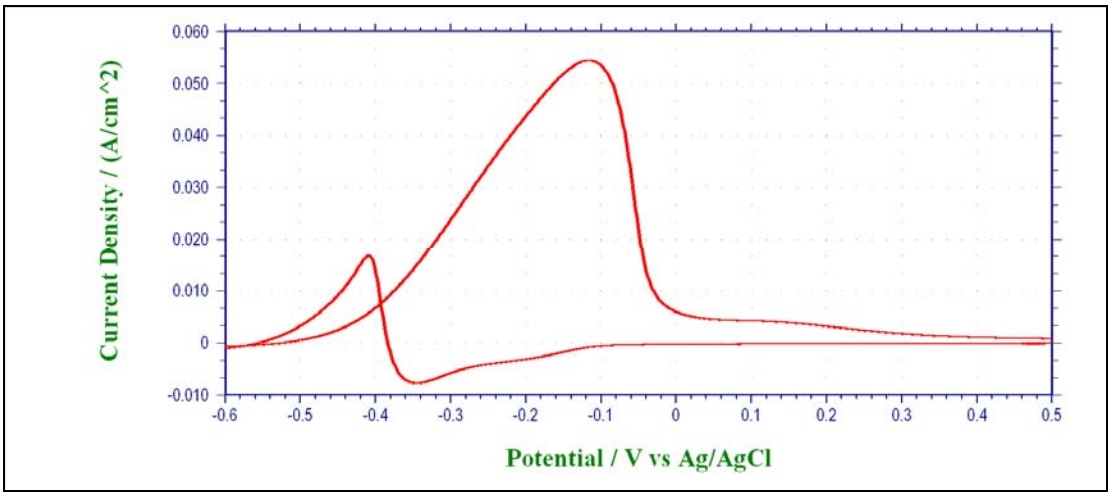

Figure 17: Cyclic voltammogram for 0.5 M ethanol on a Pt/CeO_2 composite electrode recorded in 1.0 M NaOH electrolyte at 24°C, scan rate 50 mV/s

The chemisorbed hydrogen region is suppressed due to surface blocking by decomposition products. Starting around -0.55 V vs. Ag/AgCl, the onset potential, the adsorbed decomposition products are oxidized, liberating surface sites for continuous oxidation. At higher potentials, surface oxidation takes place, blocking adsorption of the reactant and causing the oxidation current to decrease. In the cathodic sweep, the surface oxides are reduced, reactivating oxidation currents until the potential is too negative to oxidize the adsorbed species and the surface is blocked again [24]. The overall current of the modified (Pt/ceria) electrode was higher compared to the bare polycrystalline Pt electrode. The peak potential for the anodic peak was -0.12 V vs. Ag/AgCl and its current density was 0.054 A/cm^2. The peak potential of the anodic peak obtained with a bare Pt electrode was -0.2 V vs. Ag/AgCl and its current density was 0.002 A/ cm^2. Significant differences can be seen between the cyclic voltammograms of the electro-oxidation of ethanol in 0.5 M sulfuric acid and in 1.0 M sodium hydroxide. First, the

current density obtained in NaOH (0.054 A/cm^2) was higher compared to the current density obtained in the acid (0.024 A/cm^2). Secondly, the oxidation of ethanol in acidic media shows an oxidation feature at 1.1 V vs. Ag/AgCl, which was absent in alkaline media. Thus, if the CV of ethanol in acid in the potential range between 0.1 and 0.9 V were to be superimposed on the CV of ethanol in alkaline media, the CVs would show essentially the same characteristic except, as mentioned previously, the current density of ethanol in base would be higher. Additionally, the CV of ethanol in base was shifted to a more negative potential from 0.7 V to -0.12 V vs. Ag/AgCl, which represents a shift of 840 mV. Per the Nernst equation, the potential range in which water is stable shifts by -59 mV per pH unit. Dividing 840 by 59 gives 14, which is the shift in pH units when going from one end of the pH scale (0.5 M H_2SO_4 pH < 1.0) to the other end of the scale (1.0 M NaOH pH > 14). The negative shift is generally attributed to a higher affinity of OH^- for the electrode surface in alkaline media leading to a lower onset of surface oxides formation. Moreover, the shift in absolute potential strongly changes the local structure and the electric field at the electrode-electrolyte interface, subsequently causing a change in adsorption strengths [25].

4.3 Effect of Scan Rate and Ethanol Concentration

Figure 18 shows the electro-oxidation of 0.5 M ethanol in 1.0 M NaOH at five different scan rates: 25, 50, 100, 150, 200 mV/s. The cyclic voltammetry studies were also carried out at different concentrations of ethanol.

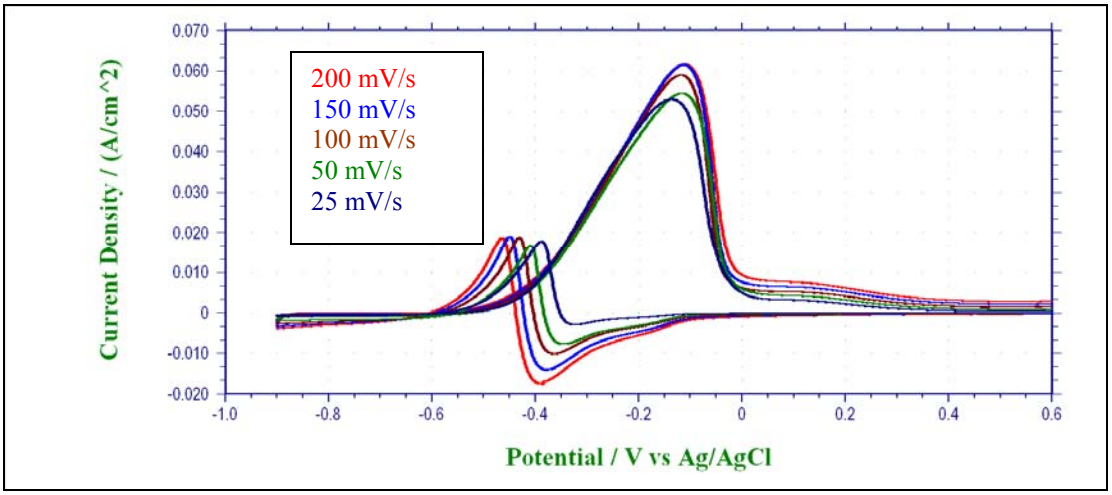

Figure 18: Cyclic voltammograms for 0.5 M ethanol on Pt/CeO_2 composite electrode in 1.0 M NaOH electrolyte at 23°C. Scan rates (v) = 200, 150, 100, 50, 25 mV/sec

For the oxidation of a 0.5 M ethanol solution in 1 M NaOH, it was observed that with increasing scan rate, the peak at potential -0.12 V did not shift in any direction with increasing scan rate and the peak currents did not increase linearly with the square root of the scan rate indicating an adsorptive process. This same pattern was observed when the ethanol concentration was changed to 1 M and 2 M. When the ethanol concentration was reduced to 0.25 M, the peak currents increased linearly with the square root of the scan rate indicating a diffusional process. However, as explained previously, at low concentrations, there is sufficient time for the CO to desorb, thus the linear relationship observed at 0.25 M is once again misleading and the process remains adsorptive at the lower concentration. Current vs. square root of the scan rate plots are shown in figures 19, 20, 21, and 22.

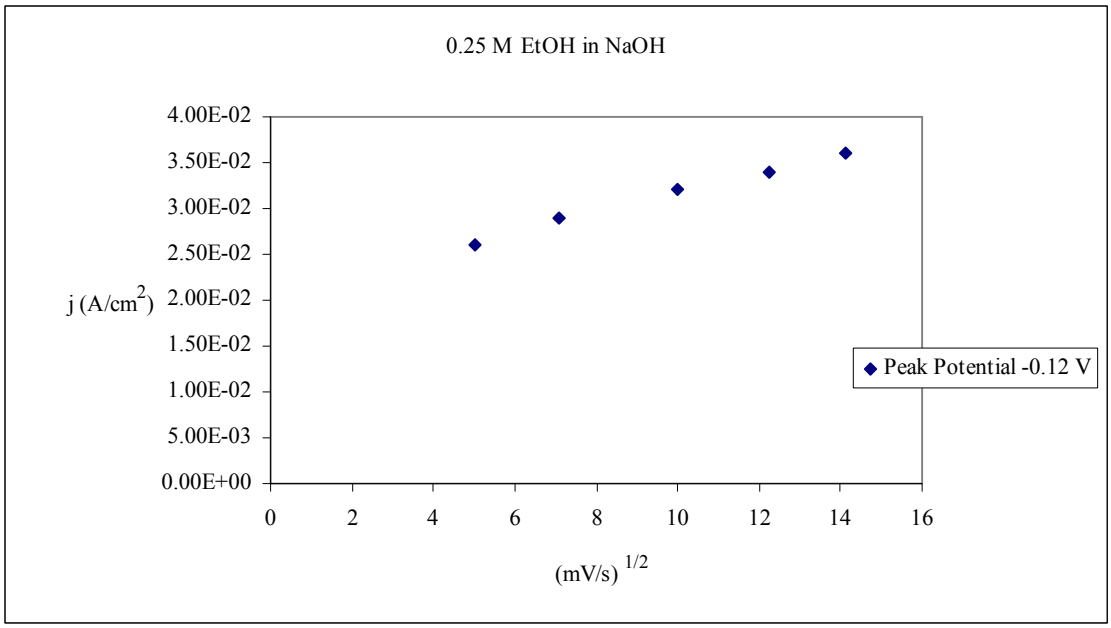

Figure 19: Peak current vs. square root of scan rate plot for 0.25 M ethanol in 1 M NaOH.

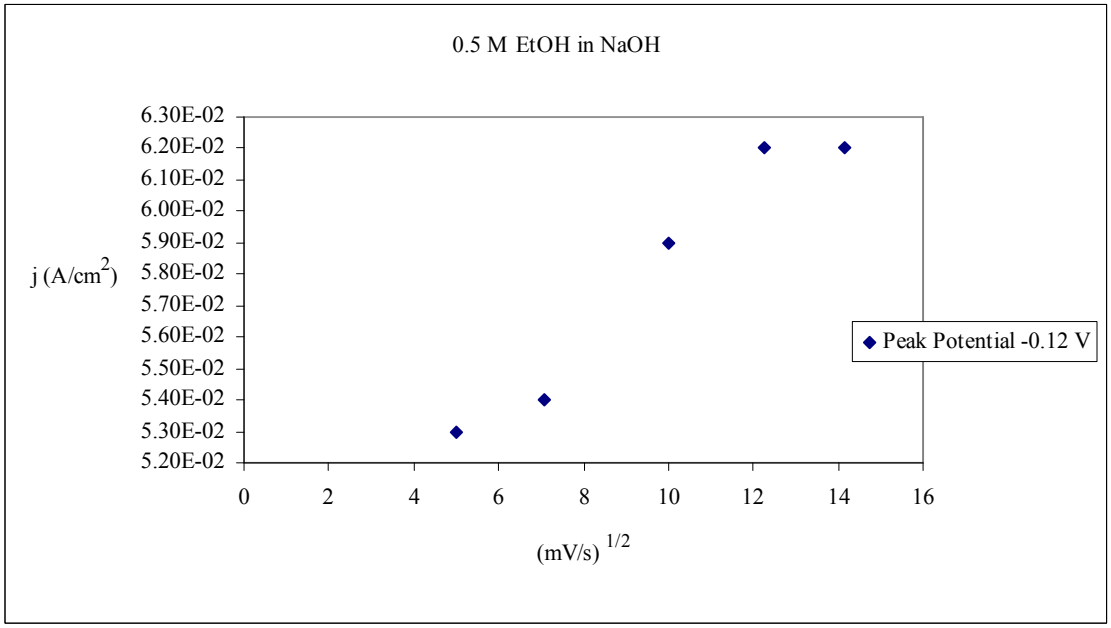

Figure 20: Peak current vs. square root of scan rate plot for 0.5 M ethanol in 1 M NaOH. The peak at potential -0.12 V is not linear with the square root of the scan rate indicating an adsorption limited reaction.

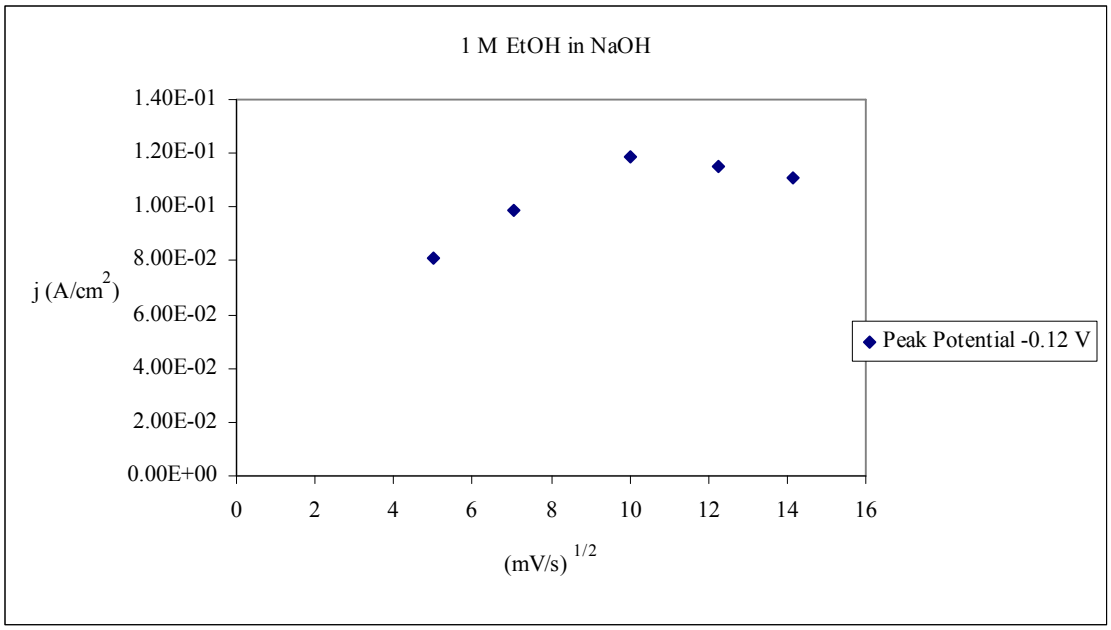

Figure 21: Peak current vs. square root of scan rate plot for 1 M ethanol in 1 M NaOH. The peak at potential -0.12 V is not linear with the square root of the scan rate indicating an adsorption limited reaction.

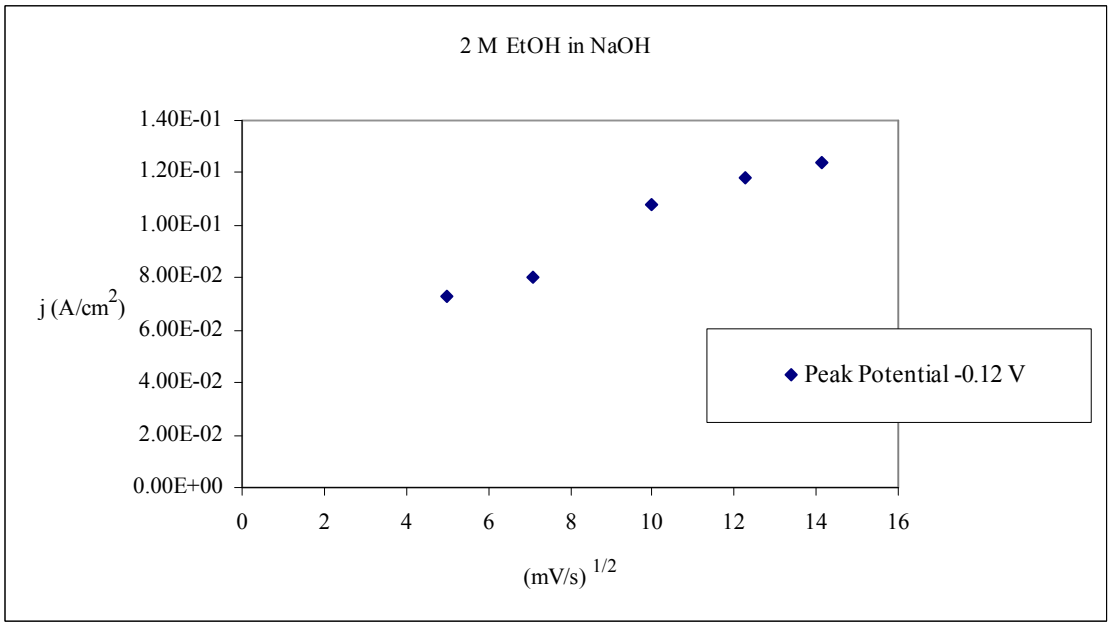

Figure 22: Peak current vs. square root of scan rate plot for 2 M ethanol in 1 M NaOH. The peak at potential -0.12 V is not linear with the square root of the scan rate indicating an adsorption limited reaction.

The peak potential of the forward anodic peak was independent of the scan rate indicating a reversible charge transport process, which was also appreciable in the cyclic voltammogram although the reaction seems to become irreversible at higher scan rates.

4.4 The Temperature Effect

Figure 23 is the I-V curves for the electro-oxidation reaction on Pt/CeO_2 composite electrode in 1 M sodium hydroxide containing 0.5 M ethanol at temperatures 15, 24, and 55°C.

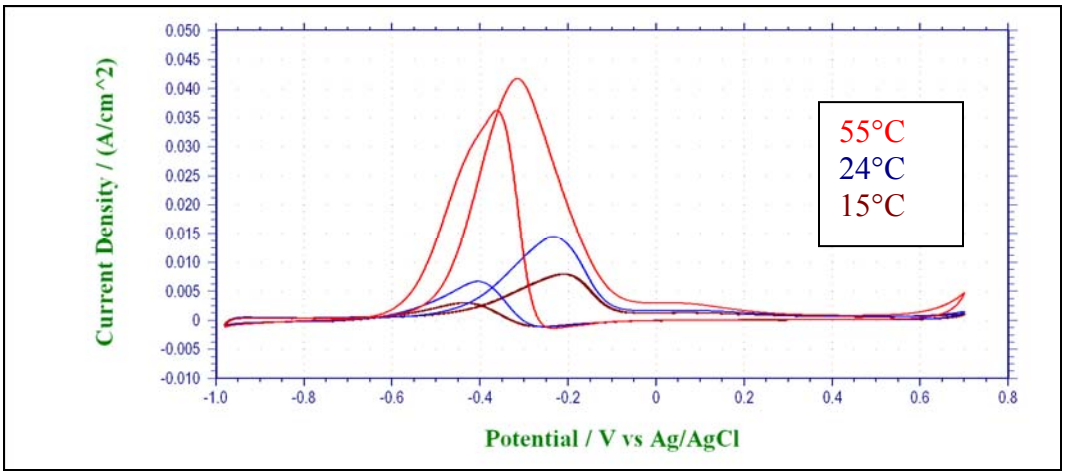

Figure 23: Cyclic voltammograms for 0.5 M ethanol on Pt/CeO_2 composite electrode in 1 M NaOH electrolyte at 15, 24, and 55°C. Scan rate (v) = 100 mV/sec

The electro-catalytic activity of the composite electrode was enhanced as evidenced by the negative shift of the onset potential and increase in oxidation current with increasing temperature. The anodic peak also becomes sharper indicating improved reaction kinetics at the higher temperature.

Figure 24 shows Arrhenius plots for the current densities obtained from the oxidation of ethanol in 1 M NaOH on a Pt/CeO_2 composite electrode at different temperatures and various potentials.

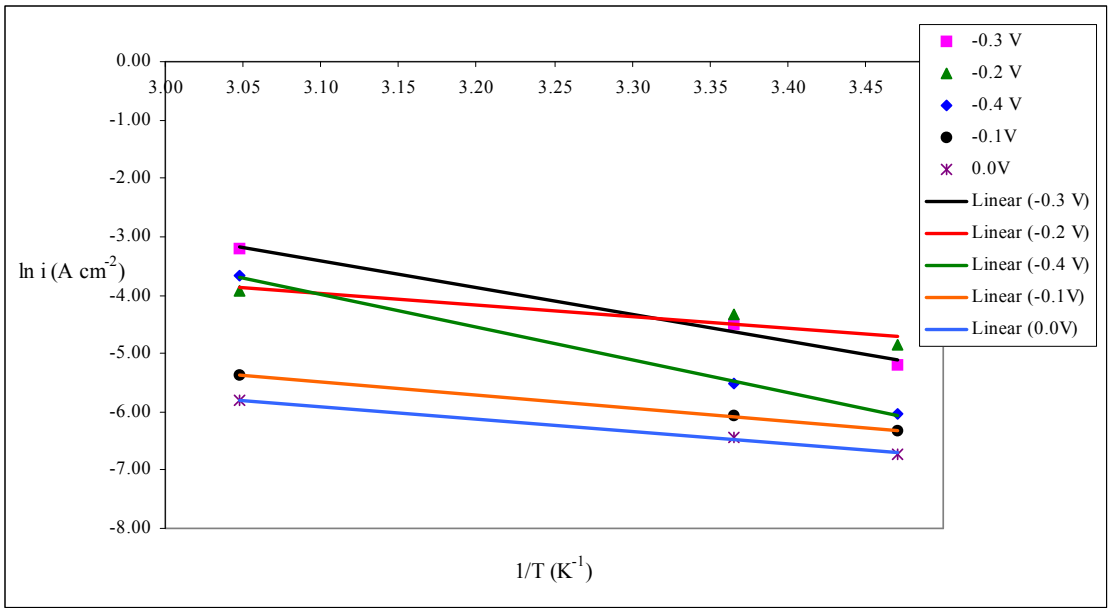

Figure 24: Arrhenius plots of for 0.5 M ethanol on Pt/CeO_2 composite electrode in 1 M NaOH electrolyte at various potentials. Scan rate (v) = 100 mV/sec.

Linear relationships were obtained at the various potentials when ln i vs. the reciprocal of the temperature was plotted. This is evidence that the mechanism at each potential was not changing with temperature. The apparent activation energies at -0.4 V, -0.3 V, -0.2 V, -0.1 V and 0.0 V were 46.7, 37.7, 16.5, 18.4, and 17.6 kJ/mol, respectively. The apparent activation energies were plotted against potential in figure 25.

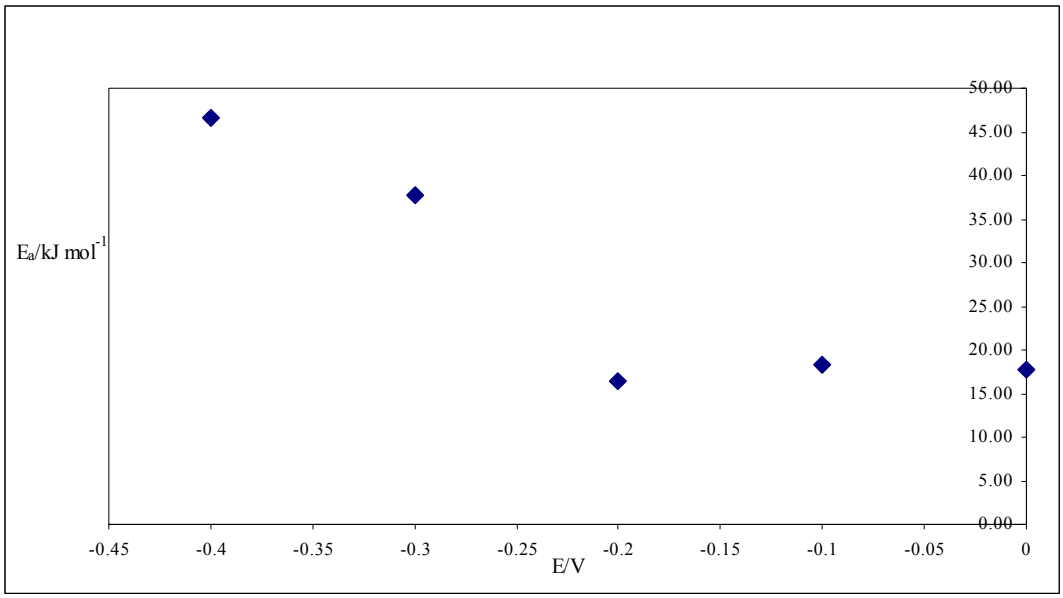

Figure 25: Apparent activation energy vs. potential for 0.5 M ethanol in 1 M NaOH. Scan rate 100 mV/second.

In a similar manner as the electro-oxidation of ethanol in acid, the plot shows a strong dependence of the apparent activation energy on the electrode potential and the apparent activation energy decreases as the potential increases. It is worthy to note that the curve in figure 25 was relatively identical to the curve obtained when E_a vs. E for the electro-oxidation of ethanol in acid was plotted (figure 10), but at more negative potentials. In both cases, the apparent activation energy was the highest at the two lowest potentials. Table 2 compares the activation energy in the potential range studied for the oxidation of ethanol in sodium hydroxide to the oxidation of ethanol in sulfuric acid. In both environments, acidic and basic, activation energies were high at low potentials and decreased as the potentials increase. The activation energies at the high potentials, greater than -0.2 V for alkaline and greater than 0.9 V in acid, were lower in sodium hydroxide than in sulfuric acid. Recent studies have shown that the oxidation of alcohols in alkaline media proceeds much easier than in acidic environment. This fact is ascribed

to a higher concentration of adsorbed hydroxyl, which plays a key role in the removal of electrode poisoning species[7].

Table 2: Potential vs. activation energy for the electro-oxidation of ethanol in 1 M NaOH and 0.5 M H_2SO_4

Potential vs. Activation Energy			
NaOH		H_2SO_4	
E	E_a	E	E_a
V	kJ/mol	V	kJ/mol
-0.4	46.7	0.7	43.7
-0.3	37.7	0.8	30.3
-0.2	16.5	0.9	22.4
-0.1	18.4	1	22.0
0	17.6	1.1	19.2

This result combined with the results of the scan rate experiments showing that an adsorptive process exists at low potentials may indicate that the adsorption step is the rate determining step. If this were the case, then the low apparent activation energies at the higher potentials may indicate a diffusion controlled mechanism, which is supported by the scan rate data obtained for the electro-oxidation of ethanol in acid.

4.5 Kinetics

The electro-oxidation of various ethanol concentrations in 1 M NaOH is shown in figure 26.

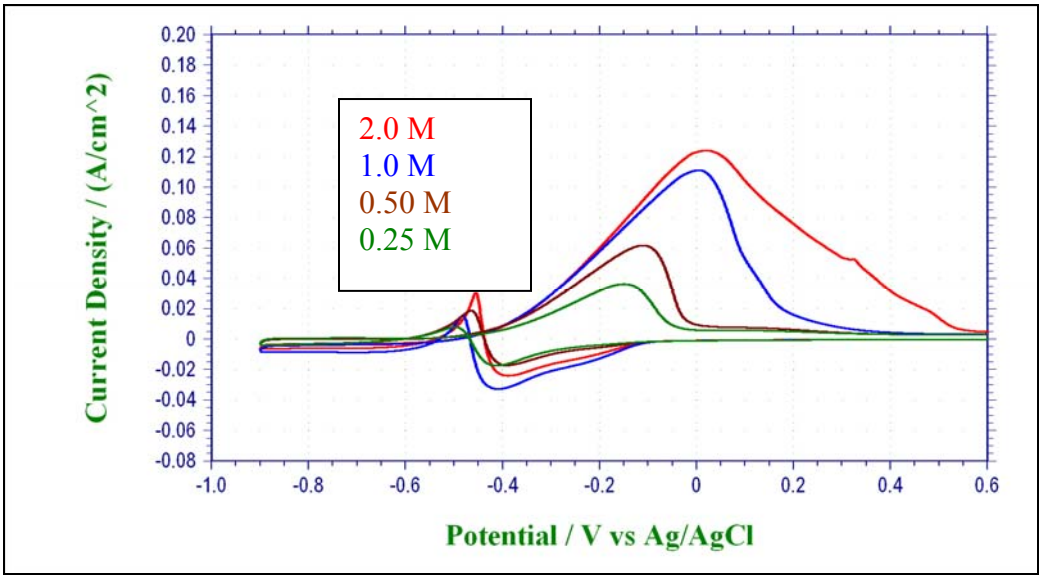

Figure 26: Voltammograms of the electro-oxidation of ethanol at 0.25 M, 0.50 M, 1.0 M, and 2.0 M in 1 M NaOH. Scan rate 200 mV/s.

As the ethanol concentration increases, the peak current densities of all peaks increase. The peaks also shift slightly positive and become broader as the concentration increases. In comparing the peak current density of the 2 M ethanol solution (0.0377 A/cm^2) to the current density of the 0.25 M ethanol solution (0.0124 A/cm^2), a decrease of almost 1 order of magnitude, there is an approximate 3 fold decrease in oxidation current similar to what is observed during the oxidation of ethanol in acid, which may indicate that the overall electro-oxidation rate is controlled by surface processes rather than by pure mass transport.

The plot of the natural logarithm of the current densities vs. the natural logarithm of the concentration of the anodic peak is shown in figure 27. The overall reaction order was m = 0.6. The reaction seems to be controlled by a half order process, which was the same result obtained in acid media.

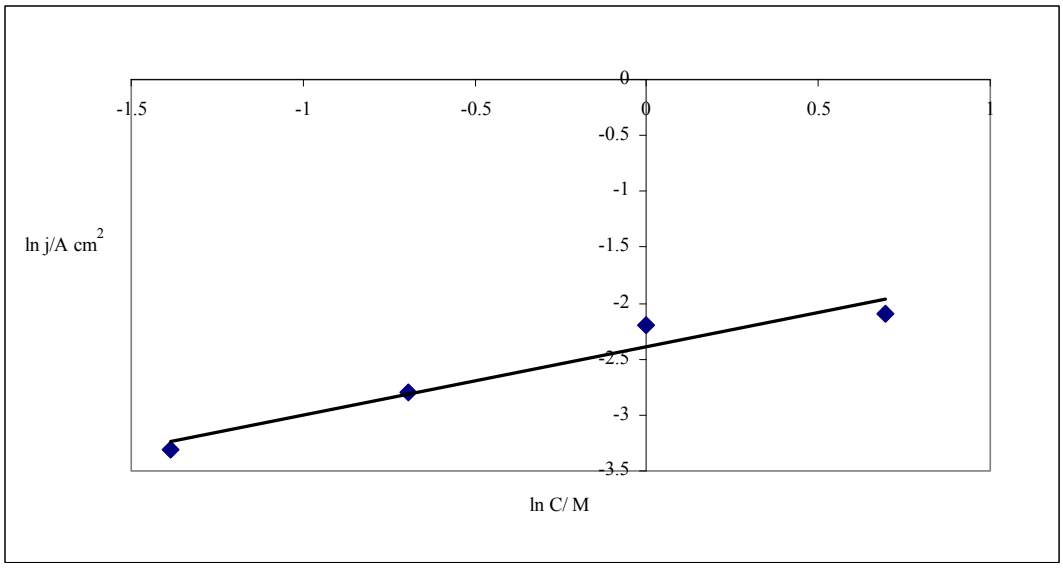

Figure 27: Plot ln j vs. ln C for the anodic peak in the electro-oxidation of ethanol at 0.25 M, 0.50 M, 1.0 M, and 2.0 M in 1 M NaOH. Scan rate 200 mV/s.

Figure 28 shows the linear sweeping voltammograms of 0.1 M ethanol in 1 M NaOH solution at the composite rotating disk electrode (RDE) at a scan rate of 5 mV/s and different rotation rates.

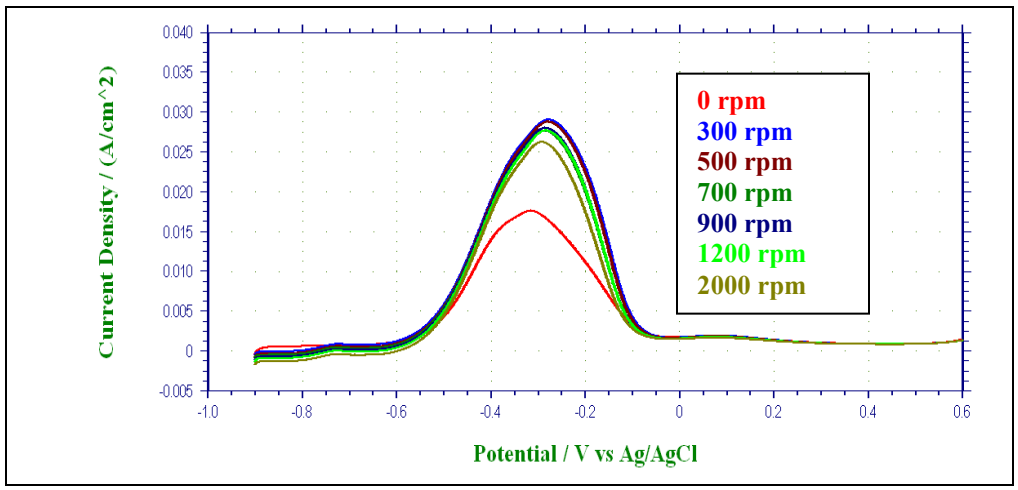

Figure 28: Linear sweep voltammograms of 0.1 M ethanol in 1 M NaOH solution at the composite rotating disc electrode at scan rate 5 mV/s with the rotation rate: 0, 300, 500, 700, 900, 1200, and 2000 rpm.

The peak current density increased when the rotation rate was increased from 0 to 300 rpm indicating a mass transport limited process. When the rotation rate was further

increased to 500 rpm, the peak current density remained constant. The peak current density decreased slightly when the rotation rate was increased to 700 rpm and stayed constant as the rotation rate was further increased to 900 and 1200 rpm indicating a kinetic limited process. An additional but small decrease was observed in the peak current density when the rotation rate was increased to 2000 rpm, but the peak current density never decreased below the current density obtained at 0 rpm as in the case of the electro-oxidation of ethanol in acid. The reaction kinetics appears to be more favorable in an alkaline media while still being kinetically limited.

5. METHANOL ELECTRO-OXIDATION ON A PLATINUM/CERIA COMPOSITE ELECTRODE IN ACID MEDIA

5.1 The Pt/ceria Composite Electrode

The cyclic voltammogram of the electro-oxidation of methanol at a Pt/CeO_2 composite electrode in 0.5 M H_2SO_4 electrolyte is shown in Figure 31 and was in good agreement with those obtained for the electro-oxidation of methanol at a polycrystalline Pt electrode [10] with one peak in the forward anodic scan and one peak in the reverse cathodic scan.

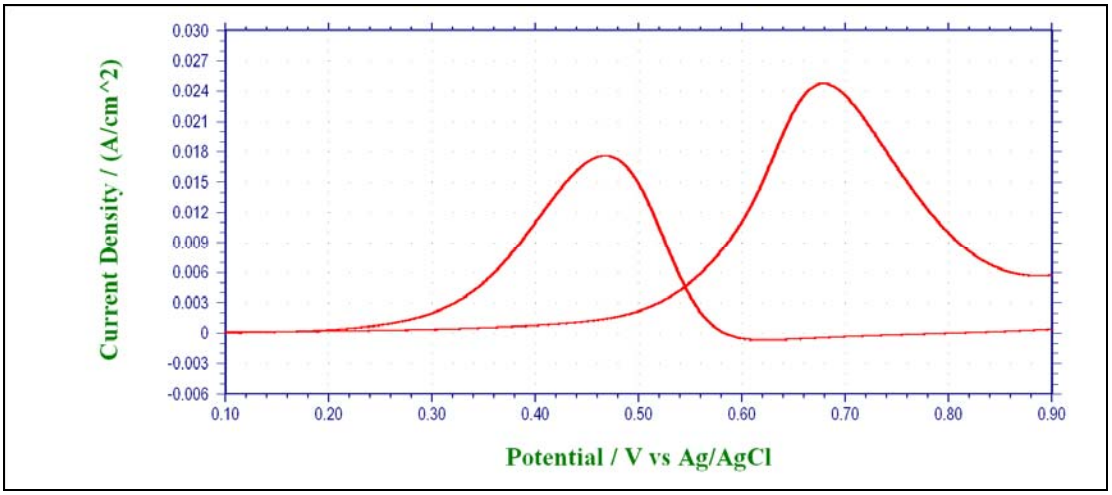

Figure 29: Cyclic voltammogram for 1 M methanol on a Pt/CeO_2 composite electrode recorded in 0.5 M H_2SO_4 electrolyte at 24 °C, scan rate 50 mV/s

At the Pt/CeO_2 composite electrode, the onset potential was approximately 0.45 V vs. Ag/AgCl. The overall current of the modified (Pt/ceria) electrode was higher compared to the bare polycrystalline Pt electrode. The peak potential for the anodic peak of the composite electrode was 0.68 V vs. Ag/AgCl and its current density was 0.025 A/cm^2. The peak potential of the anodic peak obtained with a bare Pt electrode was 0.71V vs. Ag/AgCl and its current density was 0.0004 A/cm^2.

The single carbon in methanol, and the fact that methanol is the lightest alcohol, facilitates the oxidation process of methanol to carbon monoxide, which is believed to occur via dehydrogenation of the alcohol thus accounting for the single peak in the positive scan [18]. On the forward scan, methanol oxidation was rapid between 0.5 and 0.7 V vs. Ag/AgCl. The decline in current above 0.7 V reflects the inhibition of methanol oxidation by surface oxides [26].

5.2 Effect of Scan Rate and Methanol Concentration

Figure 32 shows the electro-oxidation of 0.25 M methanol in 0.5 M H_2SO_4 at five different scan rates: 25, 50, 100, 150, and 200 mV/s. The cyclic voltammetry studies were also carried out at different concentrations of methanol.

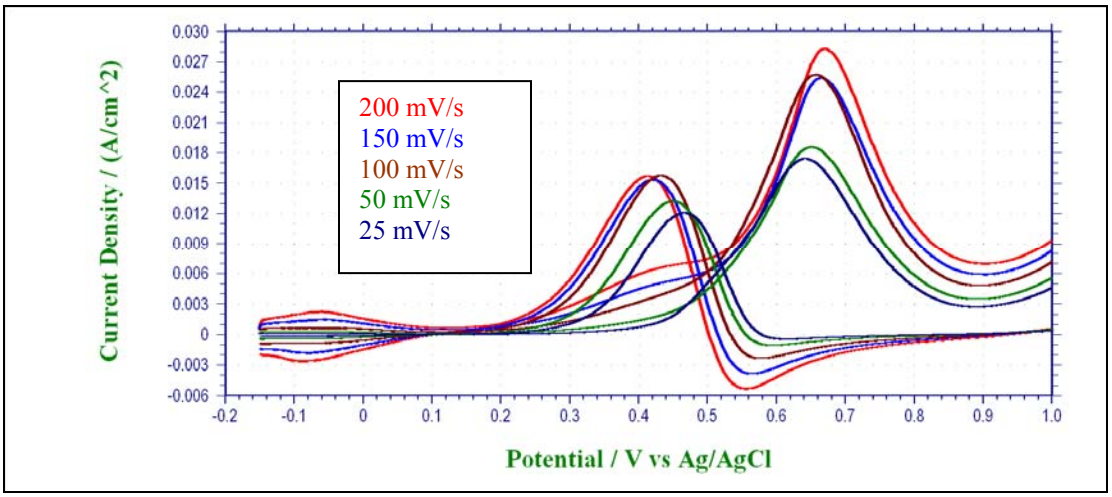

Figure 30: Cyclic voltammograms for 0.25 M methanol on Pt/CeO_2 composite electrode in 0.5 M H_2SO_4 electrolyte at 23°C. Scan rates (v) = 200, 100, 150, 50, 25 mV/sec

For the oxidation of a 0.25 M methanol solution it was observed that with increasing scan rate, the peak at potential 0.67 V shifted slightly positive except for the 200 mV/s scan rate, which remained at the same potential as the 150 mV/s scan rate. The peak currents did not increase linearly with the square root of the scan rate indicating an

adsorptive process. When the methanol concentration was increased to 0.5 M and 1 M, a linear relationship was not observed representing adsorption and thus poisoning of the electrode most likely by carbon monoxide, which is a common problem during the electro-oxidation of methanol. Current vs. square root of the scan rate plots are shown in figures 31, 32, and 33.

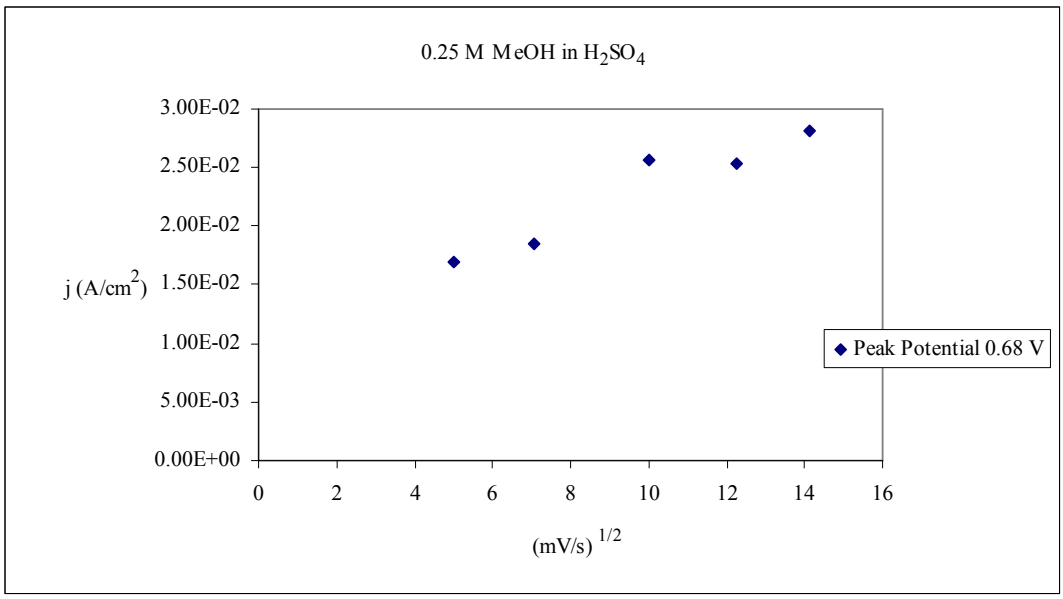

Figure 31: Peak current vs. square root of scan rate plot for 0.25 M methanol in 0.5 M H_2SO_4.

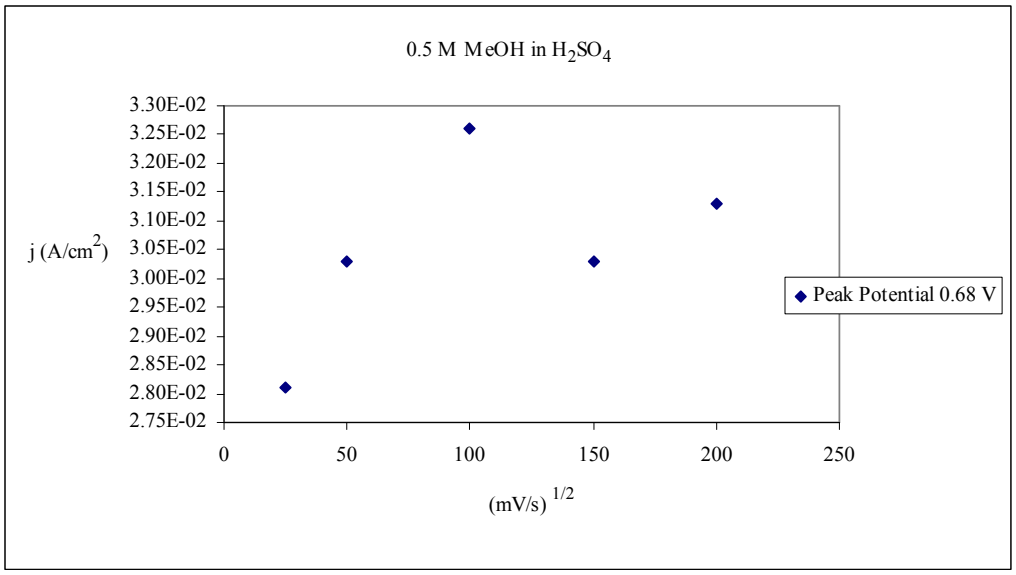

Figure 32: Peak current vs. square root of scan rate plot for 0.5 M methanol in 0.5 M H_2SO_4. The peak at potential 0.68 V is not linear with the square root of the scan rate indicating an adsorption limited reaction, which leads to poisoning of the electrode

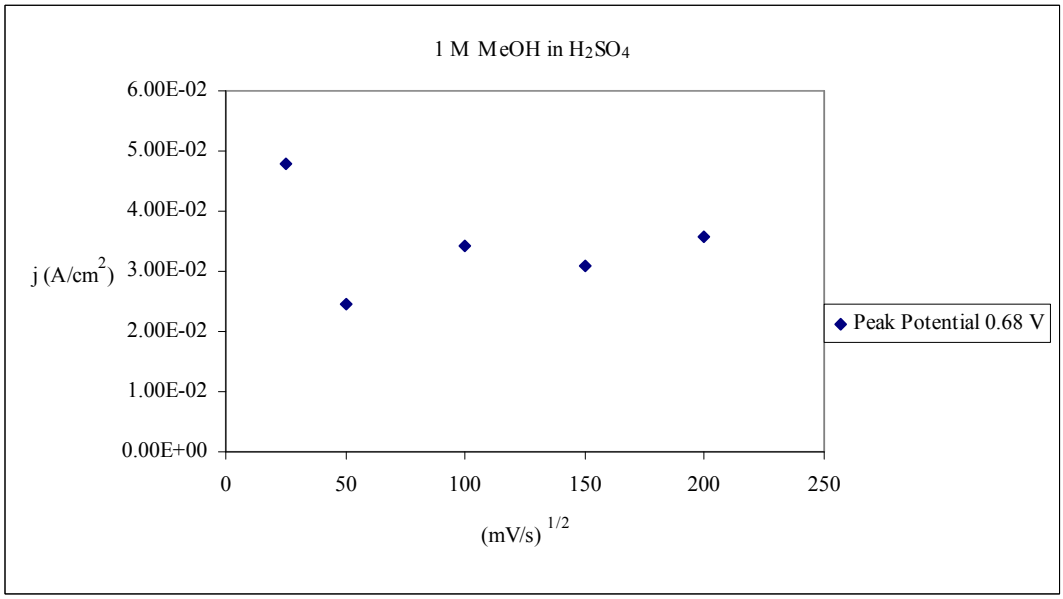

Figure 33: Peak current vs. square root of scan rate plot for 1 M methanol in 0.5 M H_2SO_4. The peak at potential 0.68 V is not linear with the square root of the scan rate indicating an adsorption limited reaction, which leads to poisoning of the electrode.

5.3 The Temperature Effect

Figure 34 is the I-V curves for the electro-oxidation reaction on Pt/CeO_2 composite electrode in 0.5 M sulfuric acid containing 0.5 M methanol at temperatures 15, 24, and 55°C.

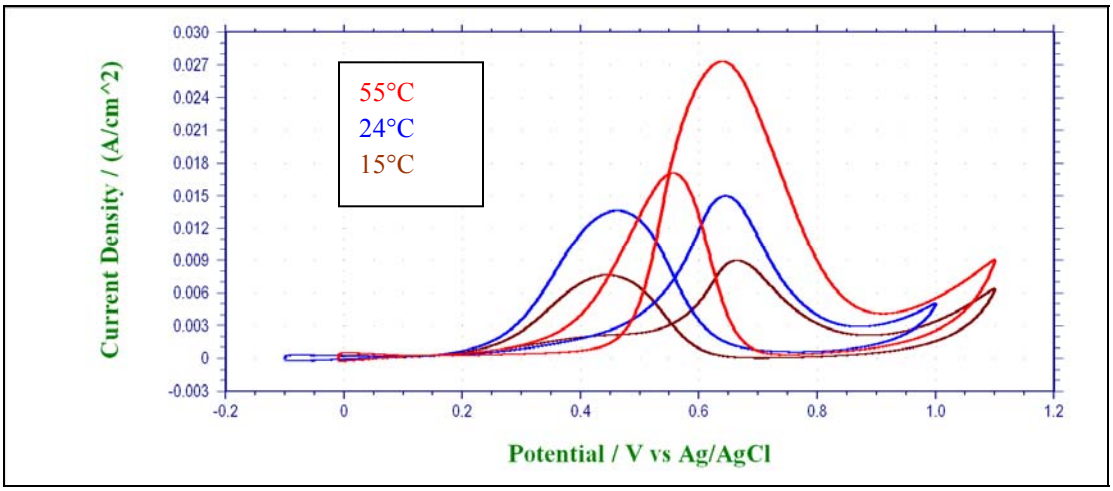

Figure 34: Cyclic voltammograms for 0.5 M methanol on Pt/CeO_2 composite electrode in 0.5 M H_2SO_4 electrolyte at 15, 24, and 55°C. Scan rate (v) = 100 mV/sec

The peak current on the forward scan was approximately three times larger at 55°C and had a wider potential range than at 24°C indicating improved reaction kinetics at higher temperatures and in agreement with previous temperature-dependent studies [26]. In contrast to the electro-oxidation of ethanol in sulfuric acid, the onset potential shifted positive with increased temperature.

Figure 35 shows Arrhenius plots for the current densities obtained from the oxidation of methanol in 0.5 M H_2SO_4 on a Pt/CeO_2 composite electrode at different temperatures and various potentials.

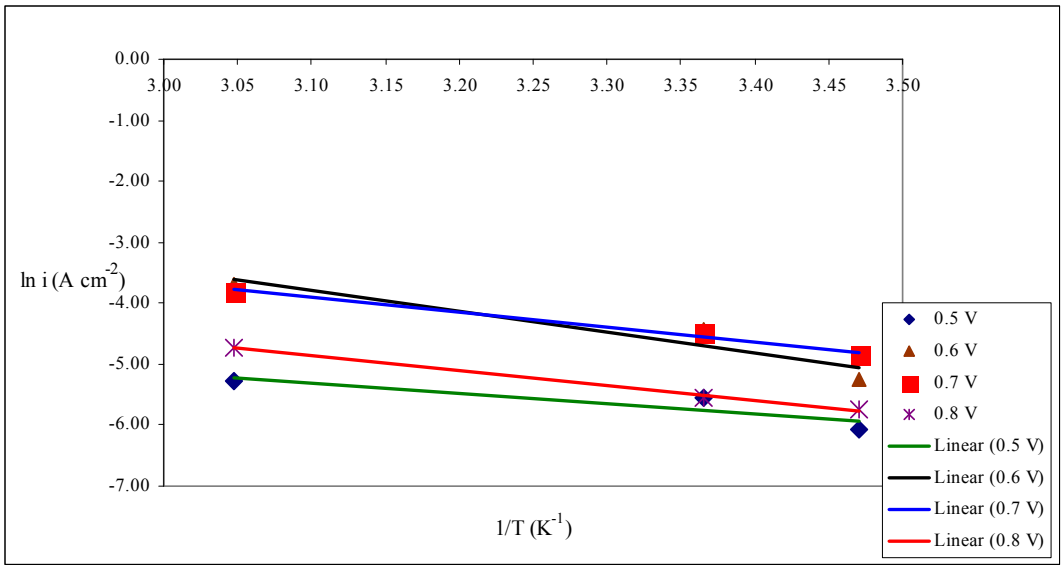

Figure 35: Arrhenius plots of for 0.5 M methanol on Pt/CeO_2 composite electrode in 0.5 M H_2SO_4 electrolyte at various potentials. Scan rate (v) = 100 mV/sec.

Linear relationships were obtained at the various potentials when ln i vs. the reciprocal of the temperature was plotted. This is evidence that the mechanism at each potential was not changing with temperature. The apparent activation energies at 0.6 V, 0.7 V and 0.8 V were 28.4, 19.9, and 20.4 kJ/mol, respectively. These values were well below the values of 44-55 kJ/mol reported for methanol adsorption on bulk Pt [27]. Kauranene et. al. reported a rough estimate for the activation energy of a carbon supported particulate Pt electrode as 16 kJ/mol [27]. The apparent activation energies were plotted against potential in figure 36.

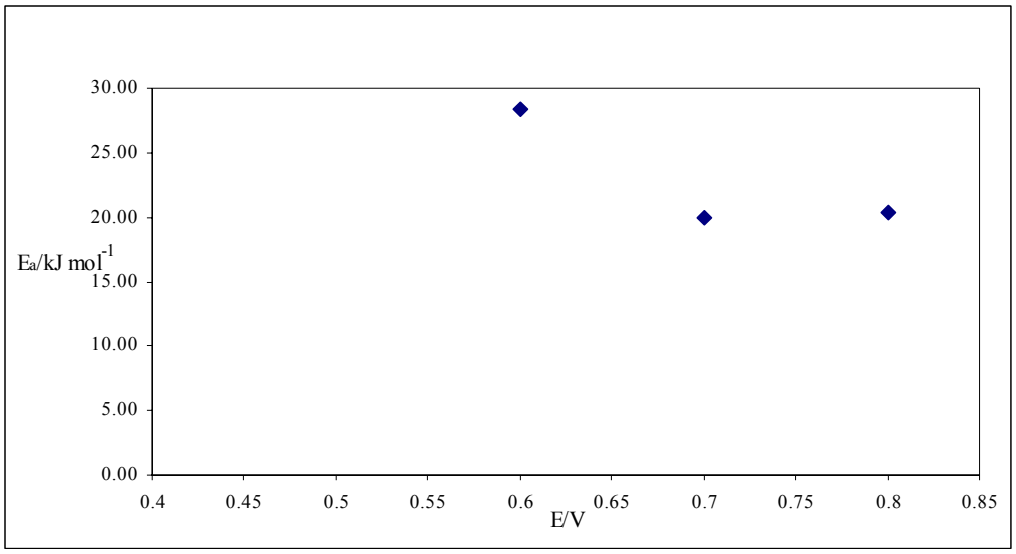

Figure 36: Apparent activation energy vs. potential for 0.5 M methanol in 0.5 M H_2SO_4. Scan rate 100 mV/sec.

5.4 Kinetics

The electro-oxidation of various methanol concentrations in 0.5 M sulfuric acid is shown in figure 37.

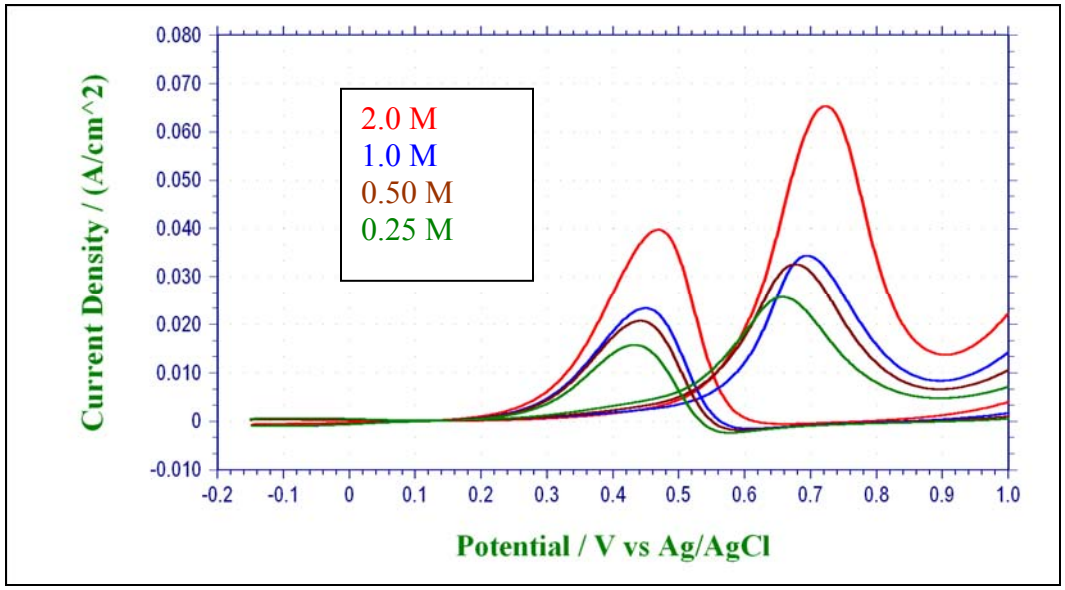

Figure 37: Voltammograms of the electro-oxidation of methanol at 0.25 M, 0.50 M, 1.0 M, and 2.0 M in 0.5 M H_2SO_4. Scan rate 100 mV/s.

As the methanol concentration was increased, the peak current densities of all peaks increased. The peaks also shifted slightly positive as the concentration increased. In

comparing the peak current density of the 2 M methanol solution (0.0652 A/cm^2) to the current density of the 0.25 M methanol solution (0.0255 A/cm^2), a decrease of almost 1 order of magnitude, there was an approximate 2.5 fold decrease in oxidation current, which may indicate that the overall electro-oxidation rate is controlled by surface processes rather than by pure mass transport.

The plot of the natural logarithm of the current densities vs. the natural logarithm of the concentration of the anodic peak is shown in figure 38. The overall reaction order was m = 0.4. The reaction seems to be controlled by a half order process, which was the same result obtained for ethanol in both acid and alkaline media.

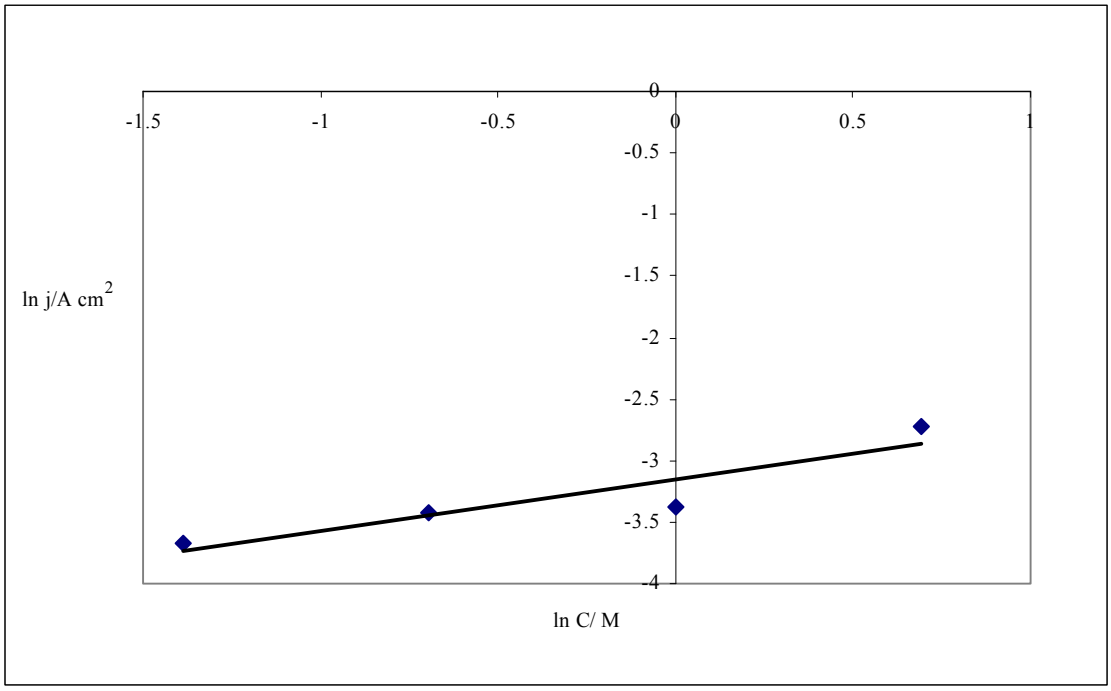

Figure 38: Plot ln j vs. ln C for the anodic peak for the electro-oxidation of methanol at 0.25 M, 0.50 M, 1.0 M, and 2.0 M in 0.5 M H_2SO_4. Scan rate 100 mV/s.

Figure 39 shows the linear sweep voltammograms of 0.1 M methanol in 0.5 M sulfuric acid solution at the composite rotating disk electrode (RDE) at a scan rate of 5 mV/s and different rotation rates.

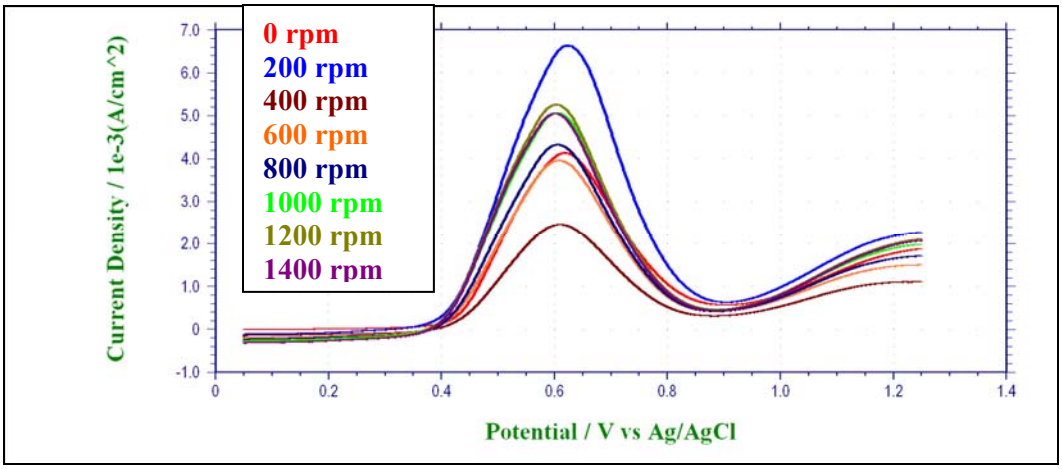

Figure 39: Linear sweep voltammograms of 0.1 M methanol in 0.5 M H_2SO_4 solution at the composite rotating disc electrode at sweep rate 5 mV/s with the rotation rate: 0, 200, 400, 600, 800, 1000, 1200, & 1400 rpm

A significant increase was observed in the current density when the rotation rate was increased from 0 to 200 rpm. When the rotation rate was increased to 400 rpm, the current density decreased to below the current density obtained when the electrode was not rotating. Rotation rates of 600 and 800 rpm produced current densities relatively similar to the current density obtained at 0 rpm. Further increase of the rotation rate caused a slight increase in the current densities. The current densities at these higher rotations, 1000, 1200, and 1400 rpm, were below the current density obtained at 200 rpm indicating slow kinetics probably due to the poisoning of the electrode by adsorbed carbon monoxide. An interesting observation was that the peak current density of approximately 6.8 x 10^{-3} A/cm^2 was relatively the same as the peak current density obtained for ethanol in acid, which was 2.8 x 10^{-3} A/cm^2. This is significant when considering the fact that a carbon-carbon bond needs to be broken in ethanol and that energy is required to break the bond. Even better results were obtained when ethanol was oxidized in NaOH. The peak current density obtained, 3.0 x 10^{-2} A/cm^2, was 1 order of magnitude higher than that of ethanol or methanol in acid.

6. METHANOL ELECTRO-OXIDATION ON A PLATINUM/CERIA COMPOSITE ELECTRODE IN ALKALINE MEDIA

6.1 The Pt/ceria Composite Electrode

The cyclic voltammogram of the electro-oxidation of methanol at a Pt/CeO_2 composite electrode in 1 M NaOH electrolyte is shown in Figure 40.

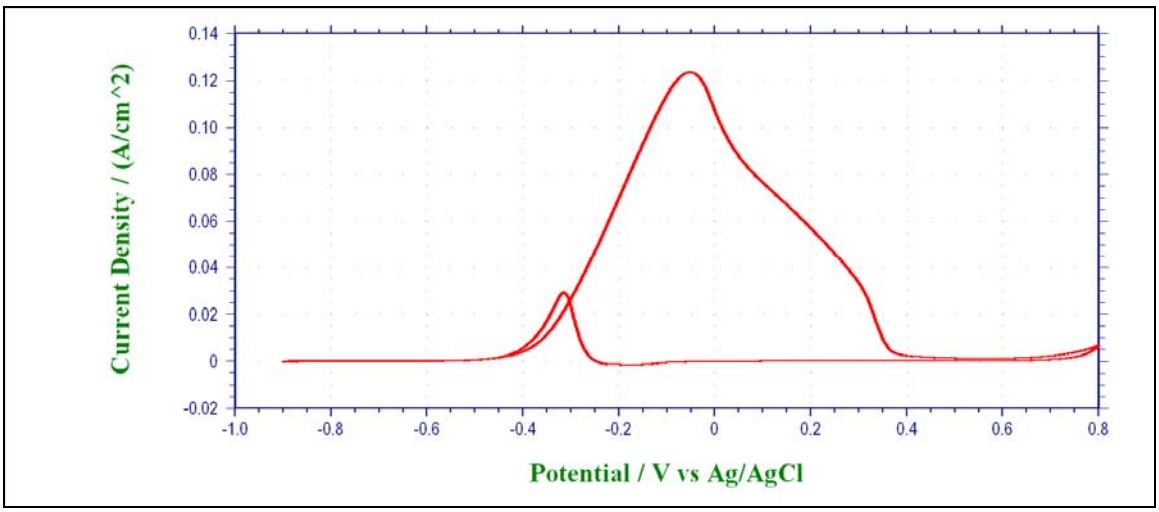

Figure 40: Cyclic voltammogram for 1 M methanol on a Pt/CeO_2 composite electrode recorded in 1 M NaOH electrolyte at 24 °C, scan rate 50 mV/s

The CV has characteristic peaks of methanol oxidation in the anodic and cathodic scans similar to those observed in the acid medium but at more negative, thus more favorable, potentials. The characteristic anodic peak being the adsorption/desorption of hydrogen followed by the reversible adsorption of the hydroxide ion, and ending with the formation of oxides. The onset potential was approximately -0.40 V vs. Ag/AgCl. The overall current of the modified (Pt/ceria) electrode was higher compared to the bare polycrystalline Pt electrode. The peak potential for the anodic peak of the composite electrode was -0.051 V vs. Ag/AgCl and its current density was 0.124 A/cm^2. The peak

potential of the anodic peak obtained with a bare Pt electrode was -0.247 V vs. Ag/AgCl and its current density was 0.0068 A/cm^2.

The ratio of the forward anodic peak current, i_f, to the reverse anodic peak current, i_r, has been used to describe the catalyst tolerance to accumulation of carbonaceous species. A higher ratio indicates more effective removal of the poisoning species on the catalyst surface[28]. Table 3 shows the anodic forward/reverse peak ratio of ethanol and methanol in sulfuric acid and sodium hydroxide.

Table 3: Comparison of anodic forward/reverse peak ratio of 1 M ethanol and 1 M methanol in 0.5 M H_2SO_4 and 1 M NaOH run at 50 mV/s

Ratio of anodic forward peak to reverse peak				
Ethanol			Methanol	
Acid		Base	Acid	Base
Peak 1	Peak 2			
0.72	0.89	4.6	1.4	4.2

The ratios indicate improved oxidation in NaOH for both ethanol and methanol as expected due to higher concentration of adsorbed hydroxyl, which plays a key role in the removal of electrode poisoning species[7]. In acid, the ratio for methanol is larger than ethanol because of the single carbon in methanol. Maiyalagan et. al. reported an anodic peak ratio for the oxidation of 1 M methanol in sulfuric acid at 50 mV/s vs. Ag/AgCl at a Pt/C and Pt/V_2O_5-C electrode as 0.90 and 1.06, respectively[28]. The Pt/ceria composite electrode has a larger ratio than the Pt/V_2O_5-C electrode showing better catalyst tolerance.

6.2 Effect of Scan Rate and Methanol Concentration

Figure 41 shows the electro-oxidation of 0.25 M methanol in 1 M NaOH at five different scan rates: 25, 50, 100, 150, and 200 mV/s. The cyclic voltammetry studies were also carried out at different concentrations of methanol.

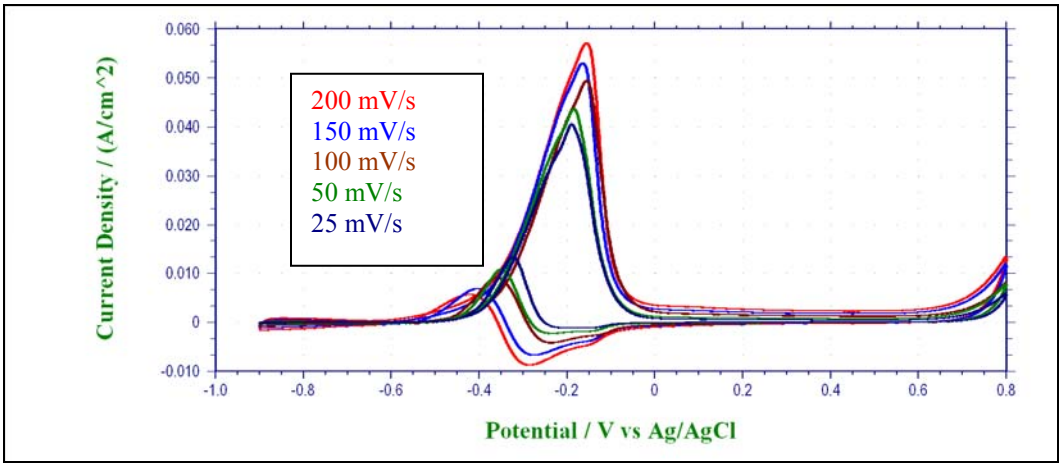

Figure 41: Cyclic voltammograms for 0.25 M methanol on Pt/CeO_2 composite electrode in 1 M NaOH electrolyte at 23°C. Scan rates (v) = 200, 100, 150, 50, 25 mV/sec

For the oxidation of a 0.25 M methanol solution it was observed that with increasing scan rate, the anodic peak remained relatively constant at a potential of -0.17 V vs. Ag/AgCl. A plot of peak current vs. the square root of the scan rate shows that the total current was proportional to the square root of the scan rate indicating a fully diffusional process. The same pattern was observed when the methanol concentration was increased to 0.5 M, 1 M, and 2 M. Current vs. square root of the scan rate plots for the different concentrations are shown in figures 42, 43, 44, and 45.

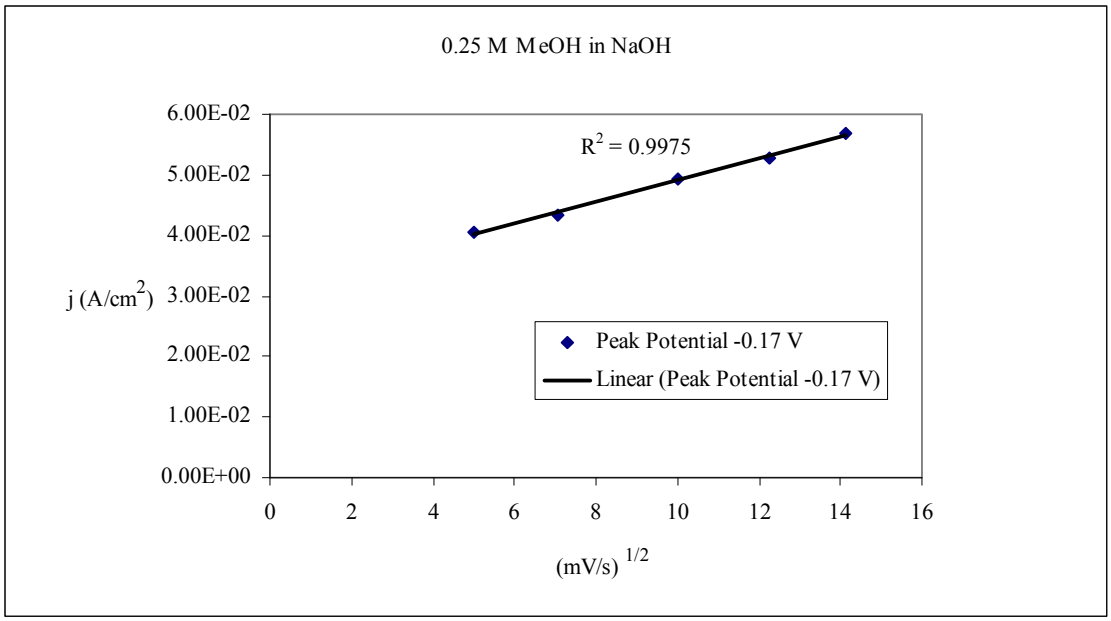

Figure 42: Peak current vs. square root of scan rate plot for 0.25 M methanol in 1 M NaOH. A linear relationship with the square root of the scan rate indicates a diffusion limited reaction.

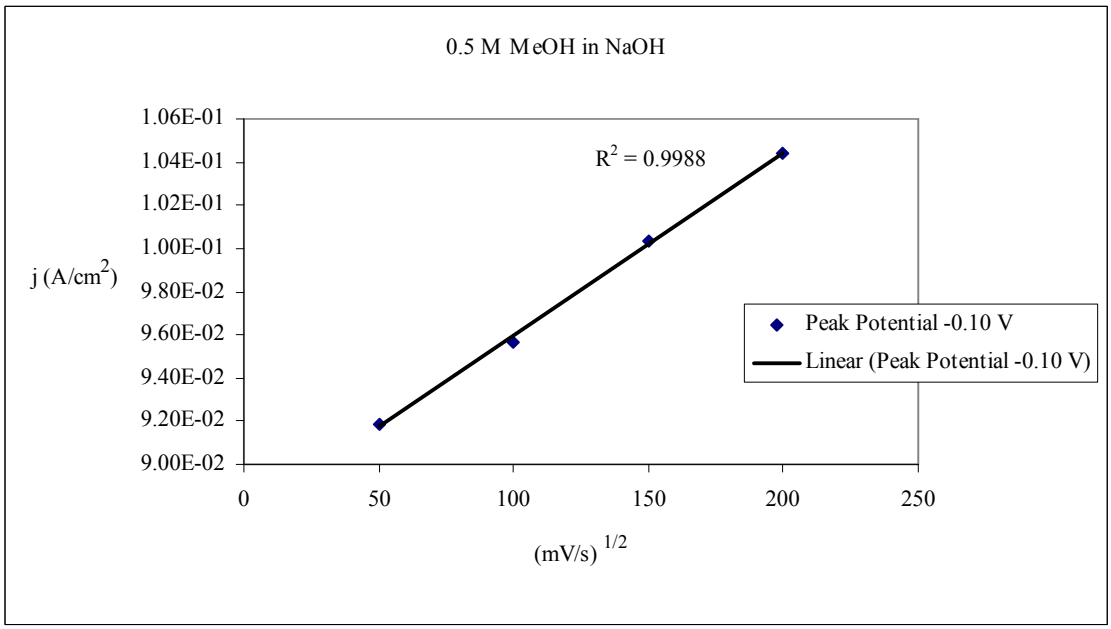

Figure 43: Peak current vs. square root of scan rate plot for 0.5 M methanol in 1 M NaOH. A linear relationship with the square root of the scan rate indicates a diffusion limited reaction.

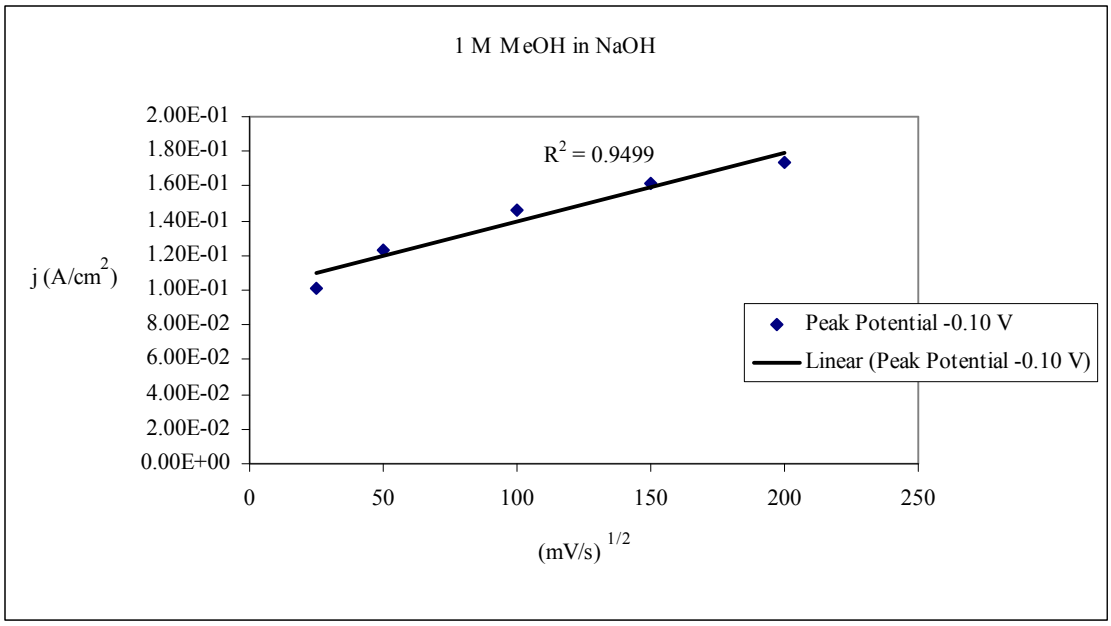

Figure 44: Peak current vs. square root of scan rate plot for 1 M methanol in 1 M NaOH. A linear relationship with the square root of the scan rate indicates a diffusion limited reaction.

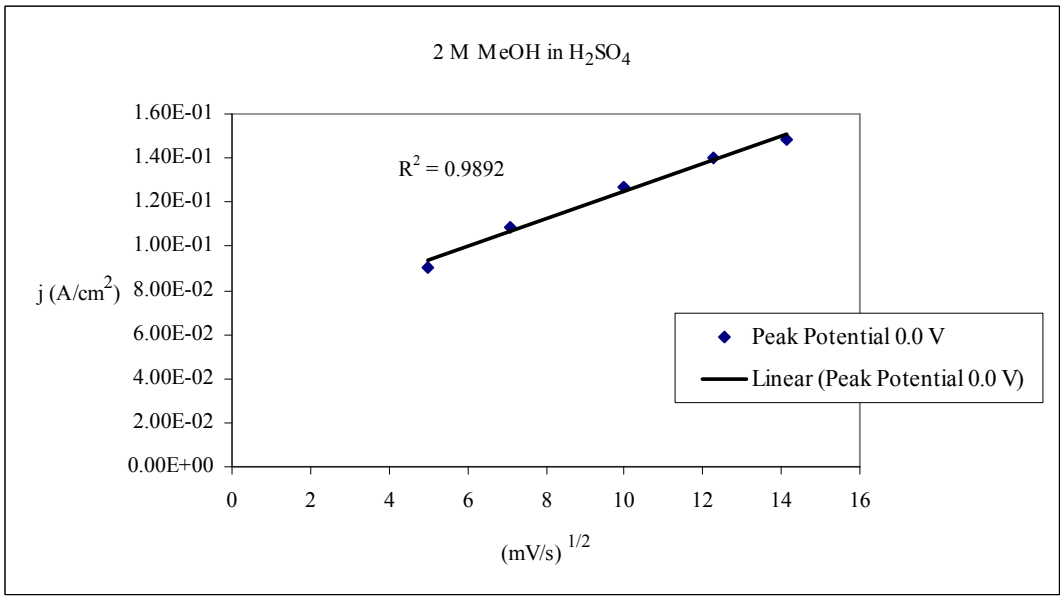

Figure 45: Peak current vs. square root of scan rate plot for 2 M methanol in 1 M NaOH. A linear relationship with the square root of the scan rate indicates a diffusion limited reaction.

Figure 46 shows the plots of peak current density vs. different concentrations of ethanol and methanol in acid and alkaline media.

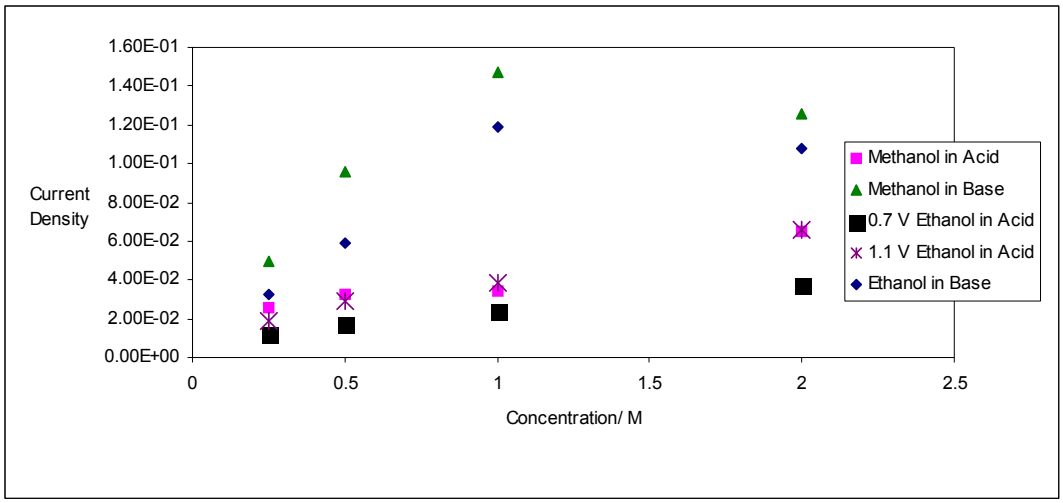

Figure 46: Plot of peak current density vs. 0.25 M, 0.5 M, 1 M, and 2 M of ethanol and methanol in 0.5 M sulfuric acid and 1 M sodium hydroxide

Improved current density was obtained for both ethanol and methanol when oxidized in basic media and saturation of the electrode was observed when the alcohol concentration was increased to 2 M. In acid media, the peak current density increased with concentration, but the current density was low compared to the current density obtained when the alcohol was oxidized in NaOH. An interesting observation was that the curve of methanol in acid and ethanol in acid at 1.1 V are in essence superimposed despite that fact that ethanol has a carbon-carbon bond. Moreover, the current densities of methanol in base and ethanol in base are in the same order of magnitude. These results indicate that ethanol may be a suitable substitute for methanol when using ceria as a co-catalyst.

6.3 The Temperature Effect

Figure 47 is the I-V curves for the electro-oxidation reaction on a Pt/CeO_2 composite electrode in 1 M sodium hydroxide containing 0.5 M methanol at temperatures 15, 24, and 55°C.

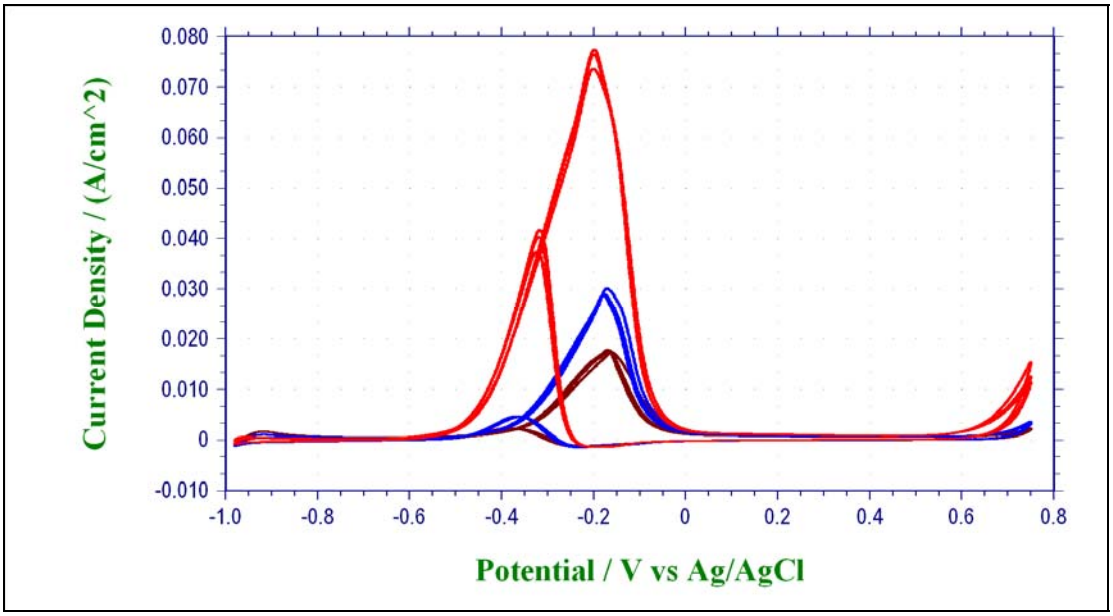

Figure 47: Cyclic voltammograms for 0.5 M methanol on Pt/CeO_2 composite electrode in 1 M NaOH electrolyte at 15, 24, and 55°C. Scan rate (v) = 100 mV/sec

The electro-catalytic activity of the composite electrode was enhanced as evidenced by the negative shift of the onset potential and increase in oxidation current with increasing temperature. The anodic peak also became sharper indicating improved reaction kinetics at the higher temperature. These results were similar to those obtained when ethanol was oxidized in NaOH although a sharper anodic peak was obtained with methanol at all three temperatures. In acid media, the onset potentials shift positive for methanol and negative for ethanol. The ceria composite electrode seems to improve ethanol oxidation in acid in agreement with the results obtained by Diaz et. al..[10] Moreover, superior reaction kinetics and electro-catalytic activity was observed when the supporting electrolyte for the ceria composite electrode was NaOH.

Figure 48 shows Arrhenius plots for the current densities obtained from the oxidation of methanol in 1 M NaOH on a Pt/CeO_2 composite electrode at different temperatures and various potentials.

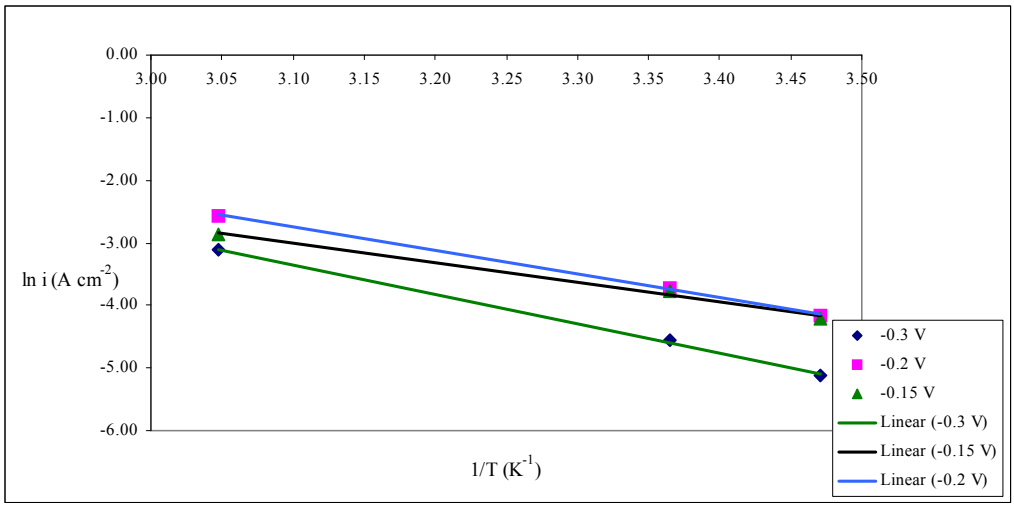

Figure 48: Arrhenius plots of for 0.5 M methanol on Pt/CeO_2 composite electrode in 1 M NaOH electrolyte at various potentials. Scan rate (v) = 100 mV/sec.

Linear relationships were obtained at the various potentials when ln i vs. the reciprocal of the temperature was plotted. This is evidence that the mechanism at each potential is not changing with temperature. The apparent activation energies at -0.3 V, -0.2 V, and -0.15 V were 39.1, 31.1, and 25.9 kJ/mol, respectively. The apparent activation energies were plotted against potential in figure 49. The plot shows a strong dependence of the apparent activation energy on the electrode potential and the apparent activation energy decreases as the potential increases.

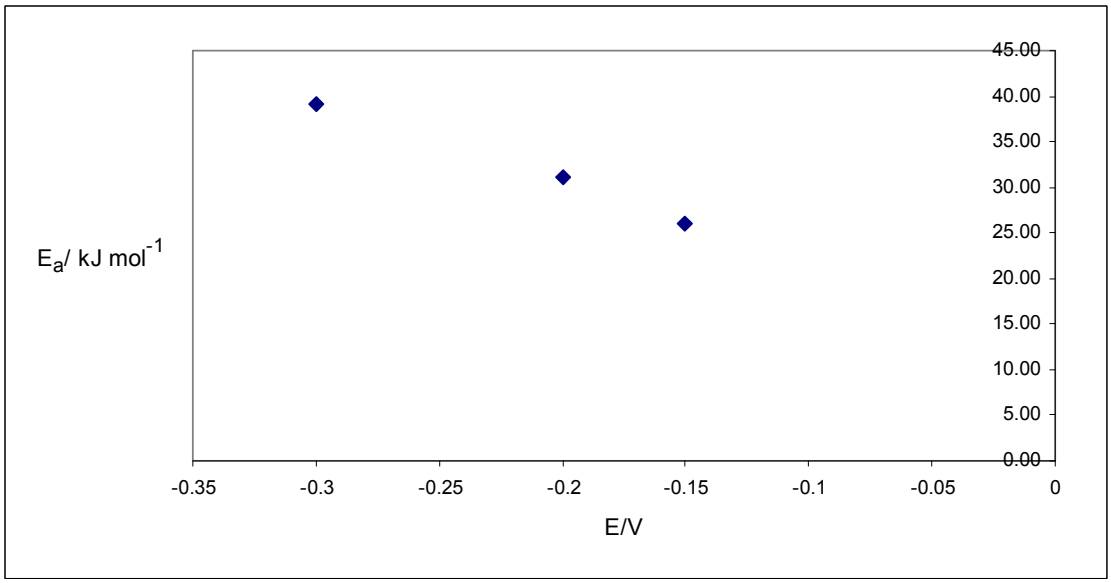

Figure 49: Apparent activation energy vs. potential plot for 0.5 methanol in 1 M NaOH. Scan rate 100 mV/sec.

6.4 Kinetics

The electro-oxidation of various methanol concentrations in 1 M NaOH is shown in figure 50.

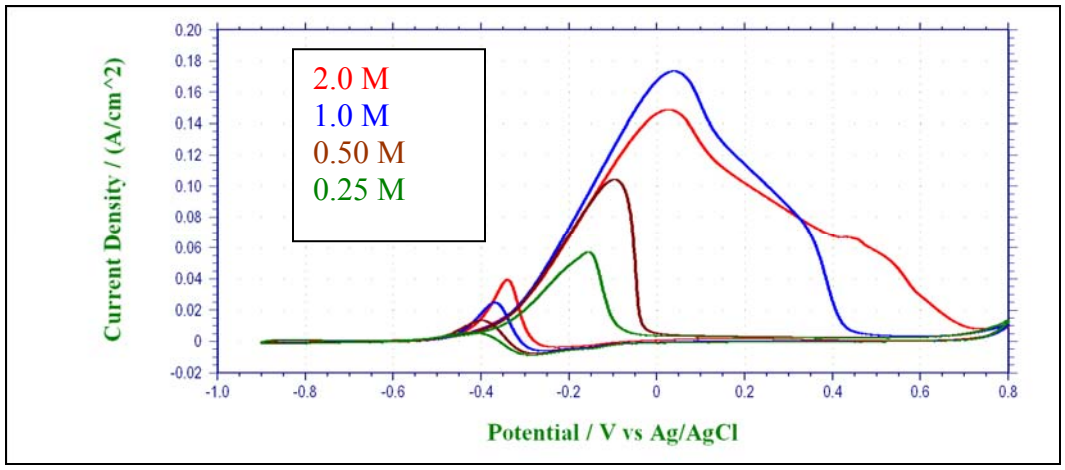

Figure 50: Voltammograms of the electro-oxidation of methanol at 0.25 M, 0.50 M, 1.0 M, and 2.0 M in 1 M NaOH. Scan rate 200 mV/s.

A positive shift was observed in the peak potential except at 2 M. Moreover, the peak current for this concentration was lower than the peak current at 1 M methanol possible indicating a saturation of the electrode. The oxidation peaks for the 0.25 M and

0.5 M were sharp peaks in relation to the 1 M and 2 M oxidation peaks, which were very broad, representative of enhanced kinetics at lower concentrations. Furthermore, as the concentration was doubled from 0.25 M to 0.5 M, the peak current density also doubled from 0.057 A/cm^2 to 0.104 A/cm^2. However when the concentration was increased by a factor of 4, from 0.25 M to 1 M, the peak current only increased by a factor of 3 from 0.057 A/cm^2 to 0.174 A/cm^2. A similar pattern was observed when the concentration was increased from 0.5 M to 1 M methanol. Even though the concentration was doubled, the peak current density only increased by a factor of 1.67. At the lower concentrations, a mass transport process dominated and at higher concentrations a surface process was dominant.

The plot of the natural logarithm of the current densities vs. the natural logarithm of the concentration of the anodic peak is shown in figure 51. The overall reaction order was m = 0.8. The reaction seems to be controlled by a first order process.

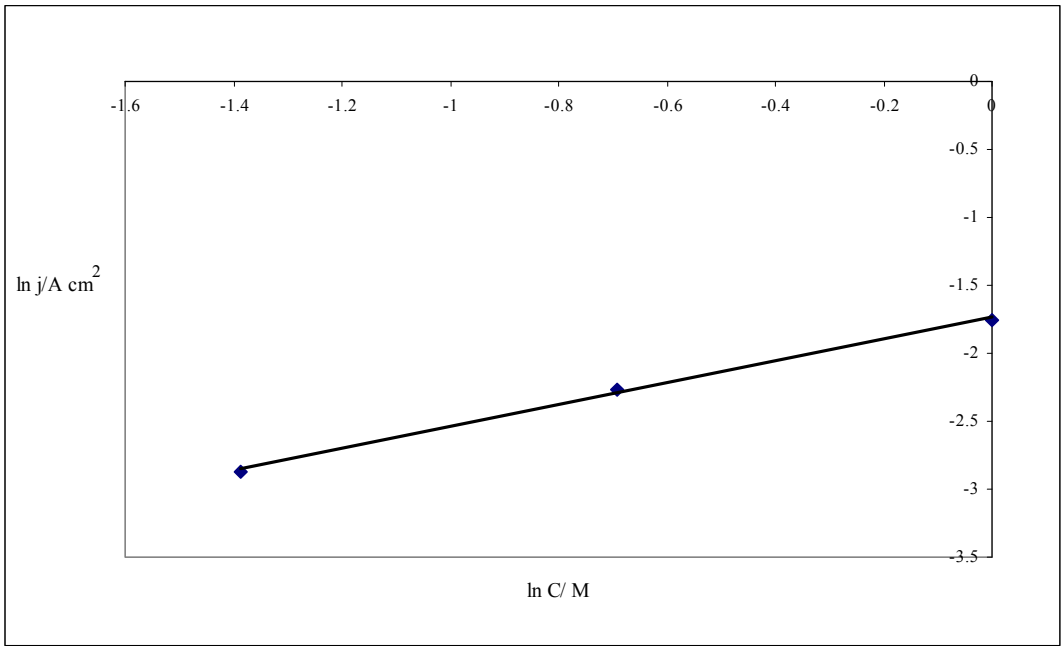

Figure 51: Plot ln j vs. ln C of the anodic peak for the electro-oxidation of methanol at 0.25 M, 0.50 M, 1.0 M, and 2.0 M in 1 M NaOH. Scan rate 200 mV/s.

Figure 52 shows the linear sweep voltammograms of 0.1 M methanol in 1 M NaOH solution at the composite rotating disk electrode (RDE) at a scan rate of 5 mV/s and different rotation rates.

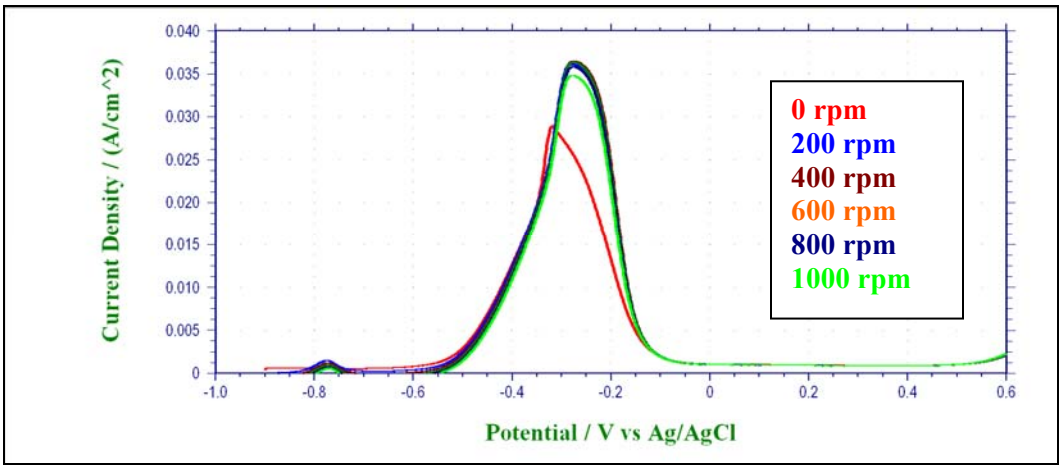

Figure 52: Linear sweep voltammograms of 0.1 M methanol in 1 M NaOH solution at the composite rotating disc electrode at sweep rate 5 mV/s with the rotation rate: 0, 200, 400, 600, 800, & 1000 rpm

The peak current density increased when the rotation rate was increased from 0 to 200 rpm indicating a mass transport limited process. When the rotation rate was further increased to 400, 600, and 800 rpm, the peak current density remained constant. The peak current density decreased slightly when the rotation rate was increased to 1000 rpm indicating a kinetic limited process. The reaction kinetics appears to be more favorable in an alkaline media while still being kinetically limited.

7. CONCLUSIONS

This study evaluated the performance of a Pt/ceria composite electrode toward the electro-oxidation of ethanol and methanol in acid and alkaline media and the following conclusions were drawn.

1) The current density for the electro-chemical oxidation at the electrode was significantly enhanced on the Pt/ceria electrode in all four instances as compared to a bare polycrystalline platinum electrode indicating the favorable electro-catalytic activity of ceria.

2) The standard rate constant for a 1 electron transfer was 4.06×10^{-4} cm/s. This value, neither large nor small, indicates more of a quasi-reversible reaction than an irreversible reaction for the electro-oxidation of ethanol in acid at the Pt/CeO_2 composite electrode.

3) The overall electro-oxidation rate was controlled by surface processes rather than by pure mass transport.

4) The electro-oxidation of ethanol in base had the lowest activation energy of all four instances. The activation energy for the electro-oxidation of ethanol in base, 18.4 kJ/mol, was lower than the activation energy for electro-oxidation of ethanol in acid, 19.3 kJ/mol, which was due to the higher concentration of adsorbed hydroxyl in an alkaline environment.

5) High activation energies were observed at low potentials for the electro-oxidation of ethanol in acid. Scan rate data for the electro-oxidation of ethanol in acid showed an adsorptive process exists at low potentials indicating that the adsorption step may be the rate determining step.

6) The highest current densities were obtained when the alcohols were oxidized in an alkaline media and alcohol concentration was 1 M. The current densities of methanol in base and ethanol in base were in the same order of magnitude.

The Pt/ceria composite electrode improved the electro-oxidation of the alcohols in the two environments studied, but the oxidation was kinetically limited. However, it was observed that the results obtained from the electro-oxidation of ethanol with the composite electrode were relatively similar to those results obtained with methanol despite the fact that ethanol has a carbon-carbon bond. For example, in the plot of current density vs. concentration (figure 46), the current density of ethanol and methanol in base were of the same order of magnitude. Moreover, the results of the linear sweep voltammetry experiments showed that the peak current density of ethanol in NaOH was higher than the peak current densities obtained for ethanol and methanol in acid. One final example is that the lowest apparent activation energy was obtained with ethanol in base. These results show that ethanol may serve as a suitable substitute for methanol as a fuel in direct alcohol fuel cells (DAFC) when using a ceria composite electrode.
The scope of future studies should include identifying the adsorbed intermediates, elucidating the reaction mechanism via spectrochemical techniques such as IR, and further kinetic evaluations of a ceria composite electrode with an additional catalyst such as rhodium.

8. REFERENCES

[1] F. Vigier, S. Rousseau, C. Coutanceau, J. Leger, and C. Lamy, Topics in Catalysis 40:111 (2006).
[2] R. L. Busby, Hydrogen and fuel cells: a comprehensive guide, PennWell Corporation, Tulsa, 2005.
[3] K. Taneda and Y. Yamazaki, Electrochimica Acta 52:1627 (2006).
[4] H. Wang, Z. Jusys, and R. J. Behm, Journal of physical chemistry B 108:19413 (2004).
[5] M. A. Scibioh, S. Kim, E. A. Cho, T. Lim, S. Hong, and H. Y. Ha, Applied Catalysis B: Environmental 84:773 (2008).
[6] R. F. B. De Souza, A. E. A. Flausino, D. C. Rascio, R. T. S. Oliveira, E. Teixeira Neto, M. L. Calegaro, and M. C. Santos, Applied Catalysis B: Environmental 91:516 (2009).
[7] D. Bayer, S. Berenger, M. Joos, C. Cremers, and J. Tubke, Internaltional Journal of Hydrogen Energy (2010).
[8] Z. Teng, Y. Wang, B. Wu, Y. Tang, T. Lu, and Y. Gao, Applied Catalysis B: Environmental 84:400 (2008).
[9] C. L. Campos, C. Roldan, M. Aponte, Y. Ishikawa, and C. Cabrera, Journal of Electroanalytical Chemistry 581:206 (2005).
[10] D. J. Diaz, N. Greenletch, A. Solanki, A. Karakoti, and S. Seal, Catalysis Letters 119:7 (2007).
[11] J. M. Dona, J. A. Herrera, and J. Perez, Journal of Chemical Education 77:3 (2000).
[12] G. A. Camara and T. Iwasita, Journal of Electroanalytical Chemistry 578:6 (2005).
[13] E. Antolini, Journal of Power Sources 170:1 (2007).
[14] S. S. Gupta and J. Datta, Journal of Electroanalytical Chemistry 594:7 (2006).
[15] C. M. A. Brett and A. M. Brett, Electrochemistry Principles, Methods, and Applications, Oxford University Press, New York, 1993.
[16] H. Wang, Z. Jusys, and R. J. Behm, Journal of Electroanalytical Chemistry 595:13 (2006).
[17] A. J. Bard and L. R. Faulkner, Electrochemical Methods Fundamentals and Applications, John Wiley & Sons, 2001.
[18] C. Lee, M. Umeda, and I. Uchida, Journal of Power Sources 160:78 (2006).
[19] Hariyanto, W. W. Purwanto, R. W-Soemantojo, and U. Stimming, Journal of Chemical and Natural Resources Engineering 2:47.
[20] H. Hitmi, E. M. Belgsir, J. Leger, C. Lamy, and R. O. Lezna, Electrochimica Acta 39:407 (1994).
[21] J. Wang, Analytical Electrochemistry, Wiley-VCH, 2000.
[22] S. B. Hall, E. A. Khudaish, and A. L. Hart, Electrochimica Acta 43:579 (1998).
[23] S. Chen and M. Schell, Electrochimica Acta 45:3069 (2000).
[24] S. Lai and M. Koper, Physical Chemistry Chemical Physics 11:10446 (2009).

[25] S. Lai, S. Kleijn, F. Ozturk, V. Vellinga, J. Koning, P. Rodriguez, and M. Koper, Catalysis Today (2010).
[26] D. Kardash and C. Korzeniewski, Langmuir 16:8419 (2000).
[27] P. S. Kauranen, E. Skou, and J. Munk, Journal of Electroanalytical Chemistry 404:1 (1996).
[28] T. Maiyalagan and F. N. Khan, Catalysis Communications 10:433 (2009).